Published in final edited form as:

Circ Res. 2020 August 14; 127(5): 631–646. doi:10.1161/CIRCRESAHA.119.315881.

CITED4 Protects Against Adverse Remodeling in Response to Physiological and Pathological Stress

Carolin Lerchenmüller[1,2,3], **Charles P. Rabolli**[1], **Ashish Yeri**[1], **Robert Kitchen**[1], **Ane M. Salvador**[1], **Laura X. Liu**[1], **Olivia Ziegler**[1], **Kirsty Danielson**[1], **Colin Platt**[1], **Ravi Shah**[1], **Federico Damilano**[1], **Piyusha Kundu**[1], **Eva Riechert**[2,3], **Hugo A. Katus**[2,3], **Jeffrey E. Saffitz**[4], **Hasmik Keshishian**[5], **Steven A. Carr**[5], **Vassilios J. Bezzerides**[6], **Saumya Das**[1], **Anthony Rosenzweig**[1]

[1]Corrigan Minehan Heart Center and Cardiology Division, Massachusetts General Hospital and Harvard Medical School, Boston, MA

[2]Cardiology Department, University Hospital Heidelberg, Heidelberg, Germany

[3]German Center for Cardiovascular Research, Partner Site Heidelberg/Mannheim, Germany

[4]Pathology Department, Beth Israel Deaconess Medical Center, Boston, MA

[5]Broad Institute of MIT and Harvard, Cambridge, MA

[6]Cardiology Department, Boston Children's Hospital, Boston, MA

Abstract

Rationale: Cardiac CITED4 is induced by exercise and is sufficient to cause physiological hypertrophy and mitigate adverse ventricular remodeling after ischemic injury. However, the role of endogenous CITED4 in response to physiological or pathological stress is unknown.

Objective: To investigate the role of CITED4 in murine models of exercise and pressure overload.

Methods and Results: We generated cardiomyocyte-specific CITED4 knockout mice (C4KO) and subjected them to an intensive swim exercise protocol as well as transverse aortic constriction (TAC). Echocardiography, western blotting, qPCR, immunohistochemistry, immunofluorescence, and transcriptional profiling for mRNA and miRNA expression were performed. Cellular crosstalk was investigated in vitro.

CITED4 deletion in cardiomyocytes did not affect baseline cardiac size or function in young adult mice. C4KO mice developed modest cardiac dysfunction and dilation in response to exercise. After TAC, C4KOs developed severe heart failure with left ventricular dilation, impaired cardiomyocyte growth accompanied by reduced mammalian target of rapamycin (mTOR) activity

Address correspondence to: Dr. Anthony Rosenzweig, Massachusetts General Hospital, Cardiology Division, GRB810, 55 Fruit Street, Boston, MA 02114, Tel: (617) 724-1430, arosenzweig@partners.org.

DISCLOSURES

SD holds a patent on microRNA 30d as a biomarker and possible therapeutic in heart failure and is a founding member of Dyrnamix, that played no role in this study.

This manuscript was sent to Elizabeth Murphy, Internal Consulting Editor, for review by expert referees, editorial decision, and final disposition.

and maladaptive cardiac remodeling with increased apoptosis, autophagy, and impaired mitochondrial signaling. Interstitial fibrosis was markedly increased in C4KO hearts after TAC. RNAseq revealed induction of a pro-fibrotic miRNA network. miR30d was decreased in C4KO hearts after TAC and mediated crosstalk between cardiomyocytes and fibroblasts to modulate fibrosis. miR30d inhibition was sufficient to increase cardiac dysfunction and fibrosis after TAC.

Conclusions: CITED4 protects against pathological cardiac remodeling by regulating mTOR activity and a network of miRNAs mediating cardiomyocyte to fibroblast crosstalk. Our findings highlight the importance of CITED4 in response to both physiological and pathological stimuli.

Graphical Abstract

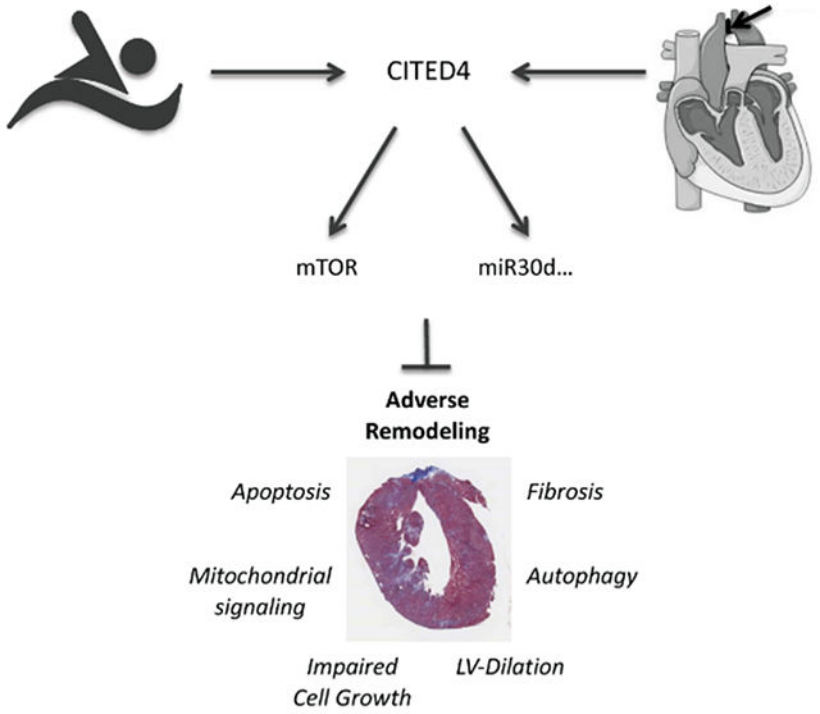

Keywords

Basic Science Research; Cardiac hypertrophy; cardiac remodeling; exercise; cell signaling; extracellular matrix

INTRODUCTION

Exercise promotes cardiovascular health and mitigates established disease.[1] Exercise training leads to an increase in cardiac mass, called physiological hypertrophy, which appears to mediate cardiac benefits.[2] In contrast, pathological stimuli, e.g. hypertension and aortic stenosis, lead to pathological growth, which often precedes heart failure and is associated with adverse outcomes. While physiological and pathological hypertrophy appear similar macro- and microscopically at early stages, the underlying mechanisms are often distinct.

Genome-wide analysis of all transcriptional components altered in exercised hearts found that CITED4 expression increased in hearts from swum mice.[3] CITED (**C**BP/p300-**I**nteracting **T**ransactivators with **E** (glutamic acid)/**D** (aspartic acid)-rich-carboxylterminal domain[4]) proteins are 22- to 27 kDa proteins, which do not have DNA-binding motifs or DNA affinity and are thought to work through binding other transcription factors (e.g. CBP/p300).[5] In the heart, CITED4 is expressed predominantly in cardiomyocytes and only at very low levels in fibroblasts or other non-cardiomyocytes.[3]

CITED4 overexpression induced hypertrophy in neonatal cardiomyocytes *in vitro*, and a high-throughput phenotypic screen of hypertrophic agonists found that neuregulin-1 (NRG1), a physiological stimulus increased in exercise, was linked to enhanced CITED4 expression.[6] Interestingly, CITED4 also promoted a physiological cardiomyocyte growth pattern *in vitro* and prevented elongation in response to pathologic hypertrophic stimuli.[6] Subsequently, we generated a transgenic mouse model with regulated, cardiomyocyte-specific CITED4 expression.[7] Increased cardiac CITED4 expression in adult mice was sufficient to induce physiological cardiac hypertrophy with increased heart weight and cardiomyocyte size as well as normal cardiac function without fibrosis.[7] CITED4 expression also enhanced functional recovery after ischemia/reperfusion injury with reduced ventricular dilation and scar size.[7]

However, overexpression models can lead to exaggerated or even nonphysiological effects, and may not reflect the role of the endogenous pathway. To understand the role of endogenous cardiomyocyte CITED4, we generated cardiomyocyte-specific CITED4 knockout mice (C4KO). C4KO mice were phenotyped at baseline and subjected to a swimming protocol as a physiological stimulus and transverse aortic constriction- (TAC-) induced pressure overload as a pathological stimulus. We found that CITED4 increases not only in response to exercise[8] but also in response to TAC. Interestingly, while cardiac morphology and function were normal at baseline in young adult C4KO mice, they manifested a maladaptive response to exercise, characterized by ventricular dilation, reduced systolic function and increased expression of fibrosis-related and pathological genes. After TAC, C4KO mice had impaired cardiac hypertrophy corresponding with decreased activation of mTOR (mammalian target of rapamycin) and mitochondrial signaling as well as increased autophagy, apoptosis, and fibrosis. RNA sequencing revealed that CITED4 regulates a network of pro-fibrotic miRNAs. One of these, miR30d, correlates with outcomes in human heart failure patients and is released in exosomes from cardiomyocytes in response to stress.[9] miR30d appeared to mediate cardiomyocyte-fibroblast cross talk and silencing of miR30d was itself sufficient to increase fibrosis and adverse cardiac remodeling after TAC similar to that seen in C4KOs. Taken together, these data demonstrate that CITED4 is upregulated in both pathological and physiological remodeling, and protects against maladaptive remodeling in both settings.

METHODS

Detailed methods and materials are in the Online Supplement. Microarray and Sequencing data have been made publicly available at the Gene Expression Omnibus (can be accessed at

GSE149584, GSE150293) and the Sequence Read Archive (can be accessed at SRA PRJNA529610).

Further data and materials that support the findings of this study are available from the authors upon reasonable request. Please also see the Major Resources Table in the Online Supplement.

RESULTS

Generation of cardiomyocyte-specific CITED4 knockout mice.

To examine the role of cardiomyocyte CITED4 *in vivo*, we generated a cardiomyocyte-specific CITED4 knockout (C4KO) mouse by breeding αMHC-Cre transgenic to CITED4 floxed (F/F Ctr) mice. C4KO mice were born in the expected Mendelian ratio and survived into adulthood. Immunoblotting for CITED4 protein was unreliable due to insufficient and inconsistent antibody quality, but qPCR revealed ~80% reduction of CITED4 mRNA expression in adult whole heart lysates (Online Figure IA). To determine whether the residual CITED4 mRNA expression in whole heart lysates reflected expression in other cell types, we isolated cardiomyocytes from C4KO and littermate controls (Online Figure IB). Successful fractionation of cells was confirmed by immunoblotting for Troponin T (Online Figure IC). CITED4 mRNA expression was reduced >98% in cardiomyocytes isolated from C4KO mice in comparison to control mice. Of note, no reduction was seen in CITED4 expression in skeletal muscle in C4KO mice confirming the specificity of deletion (Online Figure ID).

Cardiomyocyte specific CITED4 deletion does not affect baseline cardiac mass or function in young adult mice.

We first evaluated baseline cardiac function and morphology by echocardiography in 8-12 week old C4KO mice and littermate controls. No statistically significant differences were seen in fractional shortening (%FS) (Figure 1A), left ventricular mass index (LVMI, Figure 1B), or ventricular dimensions (Online Figure IE). Consistent with this, heart weight/tibia length (HW/TL, Figure 1C) and lung weight/tibia length (LW/TL, Figure 1D) ratios were not altered in C4KO mice confirming the absence of adverse cardiac remodeling or pulmonary congestion at baseline after CITED4 deletion. Moreover, there was no statistical difference in cardiomyocyte cross-sectional area in C4KO mice compared to controls (Figure 1E, 1F). There was also no statistical difference in gene expression of markers for pathological or physiological cardiac remodeling (e.g. *ANP, BNP, αMHC, βMHC, C/EBPβ*) or fibrosis markers (e.g. *Col3a1, Col5a1, Col8a1, CTGF*) in hearts from C4KO mice at baseline (Online Figure IIA, IIB). Furthermore, expression of relevant transcription factors/co-factors (e.g. *Mef2a, Mef2c, p300, GATA4*), as well as hypoxia (*Hif1, VEGFα*), autophagy (*Atg5, Beclin1*), and apoptosis (*Bcl2, Birc2*) genes was unchanged in C4KO hearts at baseline (Online Figure IIC). Collectively these data indicate that CITED4 is not necessary for normal cardiac development or maintenance of normal cardiac structure and function in the young adult heart.

Cardiomyocyte specific deletion of CITED4 in mice causes maladaptive remodeling and a functional deficit in response to endurance exercise.

To evaluate whether CITED4, which is upregulated in response to exercise training,[8] was also *necessary* for an adaptive response to endurance exercise, we carried out a ramp swimming exercise protocol in both C4KO and littermate controls. Interestingly, C4KO mice developed mildly reduced left ventricular systolic function (% Fractional Shortening) (Figure 2A) in response to exercise training. While the overall increase in heart weight normalized to tibia length was not different between C4KO and control animals (Figure 2B), cardiomyocyte cross sectional area was reduced (Figure 2C) and left ventricular dimensions increased at the end of the swimming period (Figure 2D). There was also an increase of fibrosis-related gene expression, including *Col3a1*, *Col5a1*, and *CTGF* (Figure 2E), as well as induction of markers of pathological remodeling such as *BNP*, and markers of mTOR suppression through upregulation of *DDIT4* (Figure 2F). While relatively subtle, these results stand in contrast to the more typical physiological hypertrophy, gene expression patterns, and trend toward improved function seen with exercise. Taken together, these data indicate that CITED4 is necessary for a full cardiac adaptation to endurance exercise.

Cardiomyocyte-specific deletion of CITED4 accelerates dilation and heart failure after TAC.

While CITED4 was identified in a genome-wide screen as a transcriptional co-activator increased by exercise but not by 2 weeks of TAC,[3] we found that CITED4 expression transiently increased in hearts from control animals during the initial growth response one week after TAC, suggesting that it may play a role during that critical time. (Figure 3A). To investigate the functional role of CITED4 in pressure overload-induced cardiac remodeling, we subjected C4KO and littermate controls to TAC. First, mice were followed up to eight weeks post-surgery or until they developed severe heart failure with clinical symptoms that required euthanasia (endpoint).

Echocardiography revealed an accelerated decline in cardiac function in C4KO mice after TAC compared to littermate controls (Figure 3B, 3C). C4KO mice also rapidly developed left ventricular chamber dilation (Figure 3D, 3E), and decreased relative wall thickness (Figure 3F). Of note, C4KO hearts did not undergo a hypertrophic phase in response to pressure overload suggesting that CITED4 is necessary for initial cardiac growth in response to TAC. Increased heart weight (Figure 4A) measurements confirmed altered cardiac remodeling in C4KO mice after surgery. Lung weights were also substantially increased in C4KO mice after TAC consistent with pulmonary congestion (Figure 4B). Interestingly, cardiomyocyte cross sectional area (Figure 4C) was decreased in C4KO hearts consistent with the absence of an early hypertrophic phase and the model that CITED4 is necessary for cardiomyocyte growth in response to pressure overload. Histological analyses even as early as one week after surgery revealed increased cardiac fibrosis (Figure 4D, 4E). Longitudinally sectioned hearts showed increased interstitial fibrotic tissue throughout the ventricular wall in C4KO hearts, while fibrosis was localized to the base region in control hearts (Figure 4E). Cardiomyocyte apoptosis was also increased in C4KO hearts one week after TAC compared to littermate controls (Figure 4F, 4G), without a statistically significant difference in capillary density (Online Figure IIIA). Since adverse remodeling was most

dramatic after TAC, we focused further detailed analyses and mechanistic studies on this model.

As CITED4 overexpression after ischemia-reperfusion injury induced protective activation of mTOR signaling,[7] we analyzed mTOR downstream targets in C4KO hearts after TAC. We found decreased S6 protein and 4EBP1 phosphorylation and increased Beclin1 and Lc3II protein expression, indicating decreased cellular growth and translational mTOR activity and increased autophagy in C4KO hearts one week after TAC (Figure 5A, 5B). Reduced mTORC1 activation after TAC persisted in C4KO hearts as long as 8 weeks post-surgery (Online Figure IIIB, IIIC) while mTOR signaling appeared unchanged in unstressed hearts from C4KO mice (Online Figure IIID, IIIE). Growth factor signaling usually activates mTORC1 through AKT-mediated inhibitory phosphorylation of hamartin/tuberin (TSC1/2).[10] Interestingly, phosphorylation of AKT and (AKT-dependent) TSC2 (T1462, S939) phosphorylation were upregulated in C4KO mice one week after TAC, potentially indicating compensatory feedback signaling involving mTORC2 in response to decreased mTORC1 activity (Figure 5A, 5B). Phosphorylation of S1387-TSC2 usually resulting in mTOR suppression remained unchanged in C4KO hearts after TAC when compared to controls. However, gene expression of the TSC-dependent mTORC1 suppressor REDD1 (*DDIT4*) and its homolog REDD2 (*DDIT4L*) were upregulated in C4KO hearts one week after TAC (Figure 5C). In addition, REDD1 (*DDIT4*) but not REDD2 (*DDIT4L*) was upregulated in isolated ventricular myocytes from C4KO mice at baseline and after phenylephrine (PE) stimulation (Figure 5D), providing a potential mechanism contributing to CITED4's regulation of mTORC1 signaling. These results suggest that transient CITED4 upregulation after TAC is necessary for the early growth response of the heart, while deletion of CITED4 reduces mTORC1 activation after TAC, impairs early cardiac hypertrophy and leads to accelerated heart failure with enhanced fibrosis, apoptosis, and autophagy.

Gene expression array reveals impaired mitochondrial pathways in C4KO hearts after TAC.

To better understand the pathways contributing to C4KO phenotypes, we performed microarray analyses of hearts from C4KO and littermate controls one week after TAC when the phenotypes just began to diverge in order to avoid confounding by the heart failure phenotype that develops later in these mice. Differentially expressed mRNAs ($p \leq 0.005$; fold change≥ 1.5) were subjected to hierarchical cluster analysis and displayed in a heat map (Figure 6A) and a volcano plot to highlight the most significant differences (Online Figure IVA). We also assessed differentially regulated pathways using Gene Set Enrichment Analysis (GSEA) using Gene Ontology (GO) gene sets. Interestingly, all top ten downregulated pathways were linked to mitochondria or mitochondrial function (Figure 6B), while significantly upregulated pathways included those relevant to extracellular matrix, among others (Figure 6B). The most differentially expressed genes in the combined top ten downregulated pathways were mitochondrial complex I NADH:ubiquinone oxidoreductase subunits (*NDUF*) and genes encoding for mitochondrial inner membrane related proteins (*TIMM9*, *IMMP1L*) (Online Figure IVB). Similarly, genes necessary for mitochondrial function, such as subunits of ATP synthase (e.g. *ATP5K*, *ATP8B3*, data not shown), cytochrome c oxidase (e.g. *COX7b*, *COX5a*), and relevant Complex II genes (*SDHA*, *SDHB*) were reduced in hearts from C4KO mice after TAC (Online Figure IVB). Applying

KEGG analysis, a similar gene set was significantly downregulated (Online Figure VA). KEGG-pathways enriched for these genes included oxidative phosphorylation, citrate cycle/TCA cycle, fatty acid metabolism, cardiac muscle contraction, and dilated cardiomyopathy, among others (Online Figure VB). In an independent cohort, we confirmed significant downregulation of *NDUFs1* and *NDUFv2*, both known downstream targets of the transcriptional co-activator PGC1α (*PPARGC1A)*, which was also decreased in the hearts of C4KO mice after TAC (Figure 6C). PGC1α regulates oxidative phosphorylation and fatty acid oxidation gene expression and plays a key role in mitochondrial biogenesis and metabolism in the heart.[11] Of note, PGC1α deletion was previously shown to accelerate cardiac dysfunction in response to pressure overload and its transcription is modulated by mTORC1 in other cellular systems.[12, 13] To determine if CITED4 regulates PGC1α autonomously, we investigated gene expression in isolated adult ventricular myocytes from C4KO and control animals at baseline and after PE stimulation. While we found no statistically significant difference in PGC1α or its tested downstream targets in isolated adult C4KO cardiomyocytes, we did see a trend towards a more pronounced reduction in PGC1α signaling after PE stimulation and a significant reduction in its target NDUFs1 (Online Figure VIA). C4KO mice also showed a nonsignificant trend to decreased mitochondrial DNA content, indicative of either less mitochondrial biogenesis or increased mitophagy in response to pressure overload (Online Figure VIB). Electron microscopy of heart sections, however, did not reveal consistent morphological alterations in mitochondria between C4KO and control mice after TAC, but intracellular edema and dilation of sarcotubular structures was noted particularly in some cells in the C4KO group (Online Figure VIC). While impaired mitochondrial pathways are commonly seen in heart failure, our data indicate changes in these pathways as early as one week after TAC, when most phenotypes were not significantly different from controls and overt heart failure had not developed. Thus, the accelerated and exaggerated expression changes seen in C4KO mice likely contribute to rather than reflect the more severe ventricular dysfunction that develops later in these mice.

Fibrosis-related microRNA pathways are dysregulated in C4KO hearts after TAC.

We also analyzed microRNAs (miRNAs) that were differentially expressed in C4KO hearts after TAC by RNASeq. We found that over 70% (32 out of 43) of differentially regulated miRNAs ($p \leq 0.05$; fold change≥ 1.25) were linked to fibrosis (either through Ingenuity Pathway analysis (IPA, Qiagen) and/or prior publications) (Figure 7A). Select miRNAs either up- or downregulated in C4KO hearts after TAC were validated in an independent cohort (Online Figure VIIA). These results are consistent with the most significantly upregulated pathways detected in the gene expression analysis, which included *Serpine1*, *TGFB2, TIMP3, CTGF*, *Col5a1, Col6a1, Col8a1, TIMP1*, for example, and were enriched in extracellular matrix, extracellular structure organization, biological adhesion, and extracellular matrix component pathways, among others (data not shown). We analyzed expression of fibrosis-related genes targeted by miRNAs that were differentially expressed in C4KO hearts after TAC and found inversely regulated in the transcriptome of C4KO hearts after TAC, including *Col3a1*, *Col8a1*, *Col5a1*, *TGFb2*, *CTGF* and *PDGFc*, which were validated in an independent cohort of C4KO and littermate controls (Figure 7B).

miR30 mediates crosstalk between cardiomyocytes and fibroblasts to control CITED4-dependent fibrosis.

Among the network of miRNAs differentially regulated in C4KO hearts after TAC, four members of the miR30 family were significantly downregulated when compared to littermate controls (Figure 7A, Online Figure VIIA). miR30 family members have been shown to not only provide a useful biomarker predicting the response to therapy in heart failure patients[9, 14] but also to directly regulate cardiac fibrosis by targeting *CTGF* and *PDGFc* in cardiomyocytes and fibroblasts.[15, 16] We were particularly intrigued by miR30d, as miR30d is highly expressed in cardiomyocytes and packaged in extracellular vesicles,[9] suggesting it could mediate cross-talk between cardiomyocytes and fibroblasts in our cardiomyocyte-specific genetic model. Therefore, we first confirmed significant downregulation of miR30d in an independent sample of C4KO hearts after TAC (Figure 7C). Additionally, we showed that transgenic cardiomyocyte CITED4 expression increases cardiac miR30d in vivo[7] (Figure 7C) while miR30d expression was unchanged in hearts from C4KO at baseline (Online Figure IID). To investigate the connection between miR30d and CITED4, we turned to an *in vitro* model. siRNA-mediated knockdown of CITED4 in neonatal rat ventricular myocytes (NRVM) resulted in downregulation of miR30d expression (Figure 7D), suggesting CITED4 regulates miR30d in a cell autonomous way. We next conducted conditioned media experiments to determine if CITED4 expression regulates crosstalk between cardiomyocytes and fibroblasts. Media conditioned from NRVM in which CITED4 had been knocked down contained reduced exosomal miR30d (Online Figure VIIB) and provoked an increase in extracellular matrix genes *CTGF*, *Col3a1*, *Col1a1*, as well as fibroblast-to-myofibroblast differentiation marker alpha smooth muscle actin (*ACTA2)* and proliferation marker Periostin (*POSTN*) expression in neonatal rat ventricular fibroblasts (NRVF) compared to conditioned media from NRVM treated with a scrambled siRNA (Online Figure VIIC). Results were similar in mouse embryonic fibroblasts (MEF) treated with conditioned media from NRVM in which CITED4 had been knocked down in presence of the potent fibroblast activator Transforming growth factor–β1 (TGF-β1) (Online Figure VIID). On the other hand, we observed a trend towards lower pro-fibrotic gene expression in NRVF and MEFs with conditioned media from NRVMs alone when compared to untreated fibroblasts (Online Figure VIIC and D), which was further amplified by transfer of extracellular vesicle media (Online Figure VIIIA). To confirm the role of decreased miR30d for fibroblast activation in C4 knockdown media, we overexpressed miR30d in NRVMs through a miR-mimic and found that it blocked the MEF activation seen with conditioned media from NRVMs in which CITED4 was knocked down (Figure 7E). Exploratory bioinformatic analyses revealed additional potential downstream effectors. Comparing global transcriptional changes in C4KO hearts after TAC to transcriptional changes in response to miR30d knockdown in cardiomyocytes (NRVM), we found *Serpine1* and *ITGA5* as commonly regulated pro-fibrotic genes, for example (Online Figure VIIIB), while other gene expression changes were unique in either setting (e.g. mitochondrial genes GLUL and UQCRB were only upregulated in C4KO) underscoring the complexity. Differences in the models may also account for pathways that are not common between C4KO hearts after TAC and LNA-miR30d treated NRVMs and present a limitation of this approach.

However, we found some of the pro-fibrotic miRNA network was recapitulated in C4KO mice after swimming. For example, miR-30d and miR-133b (both anti-fibrotic) were mildly decreased, while miR-376c (pro-fibrotic miRNA) was increased (Online Figure VIIIC). These data are consistent with the fibrotic mRNA expression and mildly reduced systolic function seen in C4KO mice after swimming (Figure 2A, 2E).

To further investigate how CITED4 regulates miR30d, we performed proteomic analyses to evaluate the CITED4 interactome in cardiomyocytes. Tandem mass spectrometry after isobaric tagging (iTRAQ)[17] of overexpressed CITED4 in NRVMs revealed CBP/p300 as the most highly enriched CITED4 binding partner relative to control transduced NRVMs (Online Figure IXA). Of note, an enhancer (GH08J134830) proximal to miR30d and known to regulate miR30d expression contains a binding site for p300.[18] Further miRNA promoter sequence analysis using the PROmiRNA tool[19] revealed transcription factor binding sites for p300 and known CITED4-binding partners TFAP2A and p300[20] in many of the other differentially expressed miRNAs in C4KO hearts after TAC (summarized in Online Figure IXB). Interestingly, CBP/p300 binding to CITED4 was detected exclusively in the cytoplasm of NRVMs. This could reflect the developmental stage or the quiescent state of the cells studied. Although preliminary attempts failed to identify stimuli that induced nuclear translocation *in vitro*, such pharmacological treatments obviously do not recapitulate the biology of *in vivo* pressure overload. Moreover, in collaborative studies, we have previously demonstrated that p300 can acetylate cyclophilin D, thereby altering the mitochondrial permeability transition pore (mPTP) and apoptosis[21], suggesting a relevant role for cytoplasmic p300. Taken together, these data suggest that CITED4-p300 binding in cardiomyocytes could play a significant role in the phenotypes observed through either regulation of miR30d expression and/or mitochondrial function and apoptosis.

We then asked whether reduced miR30d could contribute the phenotypes observed in C4KO after TAC *in vivo* by examining the effects of miR30d knockdown using a locked nucleic acid (LNA) antisense inhibitor specific for miR30d. LNA-antimiR30d effectively reduced cardiac miR30d expression (Figure 8A). There was no effect of LNA-antimiR30d on baseline cardiac structure and function (Figure 8B, 8C and data not shown). However, as with CITED4 deletion, depletion of miR30d dramatically accelerated the development of cardiac dysfunction after TAC (Figure 8B) as well as ventricular dilatation (Figure 8C, 8D) and pulmonary congestion (Figure 8E). Also similar to C4KO mice, interstitial fibrosis was increased in miR30d-inhibited hearts compared to control LNA-antimiR-treated animals after TAC (Figure 8F, 8G).

DISCUSSION

In this study, we provide evidence that CITED4, previously identified as a member of the gene program activated by exercise,[3, 6, 7] is also upregulated in response to pressure overload and is necessary for cardiomyocyte growth and to prevent adverse remodeling in both settings.[3, 6, 7] This suggests that CITED4 is a notable exception to the general rule that the pathways and transcriptional mechanisms involved in physiological and pathological growth of the heart are largely distinct,[3] since it appears essential in both settings. Moreover, in the

absence of this growth and other CITED4-dependent effects, signs of maladaptive remodeling are seen with both contexts.

Constitutive cardiomyocyte-specific CITED4 deletion did not affect baseline structure or function of the heart in young adult mice. However, in a ramp swimming exercise protocol, C4KO mice developed reduced systolic function and increased ventricular dilation with decreased cardiomyocyte cross sectional area. Maladaptive ventricular remodeling in C4KO after exercise was further supported by increased gene expression markers of cardiac fibrosis (e.g. *CTGF*) and pathological stress (e.g. *BNP*). Even more dramatically, C4KO mice developed accelerated heart failure in response to pressure overload induced by transverse aortic constriction (TAC), with ventricular dilatation, increased autophagy and apoptosis. The usual initial hypertrophic response to TAC was absent in C4KO mice. While C4KO heart weights were increased after TAC, this reflected an increase in left ventricular dilation rather than hypertrophy. Given Laplace's law, failure of left ventricular wall thickening as a compensatory mechanism to reduce wall stress, could contribute to ventricular dilation and ultimately failure.[2] Interestingly, prior collaborative studies demonstrated that CITED4 inhibits cardiomyocyte elongation in response to hypertrophic agonists, driving the cell morphology towards a pathological pattern *in vitro*.[6] Our current studies demonstrate that CITED4 is essential for adaptive cardiomyocyte growth *in vivo* both in response to exercise and pressure overload.

One likely contributor to impaired cardiac growth after TAC is the observed reduction in mTORC1 activation. CITED4 deletion in cardiomyocytes led to increased expression of the mTORC1 inhibitor REDD1 (DDIT4) in both the TAC and swimming models. mTORC1 is a key regulator of cardiomyocyte hypertrophy, apoptosis, autophagy, and mitochondrial structure.[22] Processes potentially underlying accelerated maladaptive ventricular remodeling in C4KO mice were similarly multifaceted. Increased apoptosis and autophagy were also present in C4KO hearts after TAC. In line with these findings, our previous work showed that CITED4 overexpression promoted adaptive ventricular remodeling after myocardial injury, increased mTORC1 activity, and mitigated autophagy and apoptosis.[7] Of note, gene products of the autophagic pathway were increased in CITED4 depleted hearts after TAC. It has been suggested that apoptosis itself is a causal component of the pathogenesis of heart failure. As few as 23 apoptotic myocytes in 10^5 were sufficient to cause lethal dilated cardiomyopathy in mice.[23] Expression profiling in NRVMs revealed upregulation of the anti-apoptotic gene Bcl2 in response to forced CITED4 expression.[7] A direct anti-apoptotic effect has further been confirmed in these cells by showing substantially reduced cardiomyocyte apoptosis after hypoxia-reoxygenation *in vitro*.[7] As noted above, the cytoplasmic binding of CBP/p300 by CITED4 could also regulate apoptosis as we have previously shown that p300 can acetylate cyclophilin D, thereby altering the mPTP and apoptosis.[21]

Transcript profiling at an early time-point after TAC further revealed impaired mitochondrial pathways. Many of the genes downregulated in our dataset are downstream targets of PGC1α, which was also repressed in C4KO hearts after TAC when compared to controls. The expression of PGC1α and its target genes is reduced in many mouse models of heart failure.[12] However, CITED4 depletion led to a further decrease of PGC1α target genes when

compared to control animals after TAC and *in vitro* in response to PE.[12] PGC1α is also regulated by mTORC1 signaling in other cellular systems and mediates mTOR's control of mitochondrial function.[13] In line with these data, PGC1α knockout mice are able to develop initial hypertrophy in response to TAC, but subsequently develop profound cardiac dysfunction and dilated cardiomyopathy characterized by compromised mitochondrial function and energy deficit.[12] However, we cannot entirely exclude the possibility that the observed downregulation of mitochondrial pathway genes downstream of PGC1α is due to a secondary effect of heart failure rather than a direct effect of CITED4 depletion. Downreguation of these pathways can occur early during pathological remodeling before overt heart failure presents.[24] Collectively, these data suggest that CITED4 affects cell growth, survival, and energy metabolism upstream of mTORC1 in cardiomyocytes in response to pressure overload. Interestingly, however, phosphorylation of upstream AKT and TSC2 were upregulated in C4KO mice after TAC, which should lead to increased mTORC1 activity. Previous studies investigating the consequences of decreased mTOR activity in an inducible mTOR knockout mouse model after pressure overload found that even a modest reduction in mTOR activity in the adult myocardium results in dilated cardiomyopathy characterized by apoptosis, autophagy, and altered mitochondrial structure, as seen in C4KO mice after TAC.[22] Even though both mTOR complexes were affected in this model, AKT phosphorylation (an mTORC2 substrate) was also increased in mTOR knockout mice.[22] In C4KO mice, the increase in AKT phosphorylation may reflect disinhibition of mTORC2 as a result of reduced mTORC1 activity, but could also indicate the presence of another activated kinase, as speculated with mTOR knockout.[25] In any event, increased AKT and TSC2 phosphorylation suggest CITED4 regulates mTORC1 downstream of AKT and TSC2. Two potential mediators of this inhibition emerged from our expression profile: REDD1 and REDD2. Both REDD1 (*DDIT4*)[10] and REDD2 (*DDIT4L*)[26] function as mTORC1 suppressors while simultaneously increasing upstream mTORC2 signaling. REDD1 releases TSC2 from its growth-factor-induced association with inhibitory 14-3-3 proteins irrespective of TSC2's AKT-dependent phosphorylation. REDD1 is necessary for hypoxia-stimulated mTORC1 inhibition[10] and increased in C4KO mice after TAC. REDD2 is activated by pathological stress in the heart, leading to inhibition of mTORC1 signaling and increased autophagy while upstream signaling is upregulated.[26] REDD2 is increased ~2.2fold in C4KO hearts after TAC. Of note, overexpression of REDD2 in turn leads to decreased *CITED4* expression.[26] Further in vitro experimentation showed REDD1 to be upregulated in ventricular myocytes at baseline and more pronounced in response to phenylephrine stimulation, indicating an effect of CITED4 on REDD1 independent of established cardiac injury *in vivo*. REDD2 was predominantly upregulated *in vivo* in C4KO mice and not *in vitro*. One limitation of our study is that our data do not prove a causal role for changes in mTORC1 and mitochondrial pathways. However, mTORC1-inhibition and a reduction in PGC1α signaling occur earlier and are exaggerated in C4KO mice, suggesting they likely contribute to the accelerated ventricular dysfunction seen in C4KO mice after TAC. While the phenotype observed in C4KO mice after TAC shows similarity to mTOR knockout mice as noted above,[22] we acknowledge that mTOR manipulation can causes different phenotypes depending on important technical differences in the model investigated, as well as the specific molecular manipulation, timing, and degree of activation/inhibition.[25] Finally, in

C4KO, these alterations in mTOR signaling also occur in the context of other important gene network changes that likely act in combination to produce the phenotypes observed.

Of particular interest was the profound fibrosis that developed in the ventricular wall in C4KO hearts after TAC. While this could be a consequence of increased mechanical stress or increased tissue loss through apoptosis and reduced cell size requiring tissue replacement, [27] results from small RNAseq profiling led us to further investigate fibrosis related pathways in C4KO mice after TAC. Over 70% of differentially expressed miRNAs were linked to organ fibrosis. Many of those miRNAs had predicted or validated target genes that were inversely altered in the transcriptome of C4KO hearts, including *Col3a1*, *Col8a1*, *Col5a1*, *TGFb2*, *CTGF* and *PDGFc*. Interestingly, among the most differential miRNAs were members of the miR133 and miR30 family, both consistently downregulated in several models of pathological hypertrophy and heart failure and previously shown to regulate fibrosis, including the expression of CTGF in fibroblasts.[15] miR30d is highly expressed in cardiomyocytes and packaged in extracellular vesicles,[9] suggesting it could mediate crosstalk between cardiomyocytes and fibroblasts. We turned to an *in vitro* model and investigated whether CITED4-dependent miR30 reduction in NRVMs and consequently reduced exosomal miR30d would influence fibroblast extracellular matrix gene expression levels. Indeed, cardiomyocyte CITED4 silencing led to reduced miR30d expression and further experiments revealed that conditioned media from these cells provoked an increase in fibroblast *CTGF* and collagen levels. Alpha smooth muscle actin (*acta2*) as a marker for fibroblast to myofibroblast transformation and periostin (*postn*) as a marker for fibroblast proliferation were also increased in fibroblasts after treatment with conditioned media from CITED4 depleted cardiomyocytes. Inducing miR30d in the context of CITED4 knockdown in NRVMs antagonizes fibroblast activation induced by CITED4 knockdown media alone. These results suggest that miR30d mediates crosstalk between cardiomyocytes and fibroblasts dependent on CITED4, and could contribute to the increased fibrosis seen *in vivo* though likely in concert with other miR-30 family members and pro-fibrotic miRNA changes observed. In support of the relevance of our findings, miR30d depletion *in vivo*, led to rapid heart failure and cardiac fibrosis in a murine TAC model similar to that seen in C4KO mice.

As noted, while we have here demonstrated the functional relevance of miR30d, our *in vivo* results show that cardiac loss of CITED4 disturbs a whole panel of miRNAs involved in the regulation of fibrosis and previously linked to fibrotic diseases. For example, a role in cardiac fibrosis has been established for miR21, miR133, miR708, miR101, and miR29,[15, 28–35] miRNAs that were also differentially regulated in C4KO hearts after TAC. Therefore, it is unlikely that any one miRNA accounts fully for the fibrosis seen in C4KO hearts after TAC. Interestingly, some significantly downregulated miRNAs, including miR30 family members, and miR101a, and miR181, are predicted to target REDD1 and could thereby also influence the cell autonomous effect in C4KO cardiomyocytes as described above. Moreover, some miRNAs in our dataset share promoter sequences with regulatory elements and gene enhancers that bind CITED4 (e.g. EP300, TFAP2). Further investigation is warranted to understand how CITED4 regulates the expression of miRNAs.

We conclude that CITED4 is upregulated in response to both physiological and pathological stimuli, and is necessary for adaptive cardiomyocyte growth as well as to prevent adverse remodeling in both settings. These findings reveal an important role of CITED4 as a central regulator of cardiac homeostasis in the adult heart and a common node controlling cardiac growth, adaptation, and fibrosis in vivo.

Supplementary Material

Refer to Web version on PubMed Central for supplementary material.

ACKNOWLEDGMENTS

We thank Peter Lichter, Jan Gronych, Björn Tews, and Alexandros Vegiopoulos for CITED4 floxed mice and Dale Abel for αMHC-Cre mice. We thank Chunyang Xiao for carrying out surgical procedures, Yoshiko Iwamoto for assistance with immunohistochemistry, and Ling Li and Chiara Heß for technical assistance. Electron microscopy was performed at the EM Core Facility of Heidelberg University, we'd like to acknowledge their technical assistance. We thank Mirko Völkers for providing resources and fruitful discussions. Finally, we would like to thank Dr. Hang Lee for supporting statistical analyses.

SOURCES OF FUNDING

CL was funded by the German Research Foundation (DFG, LE 3257 1-1) and received support from the Medical Faculty of the University of Heidelberg via the Olympia Morata Program. CPR was supported by the American Heart Association's Founders Affiliate Undergraduate Student Summer Fellowship Program. This research was supported by grants to AR from the NIH (R01HL110733, R01HL122987, R01HL135886, R01AG061034) and the American Heart Association (16SFRN31720000), and grants to SD from the NIH (R01HL122547) and American Heart Association (16SFRN31720000). This work was further conducted with support from Harvard Catalyst (for the Harvard Catalyst Statistical Consulting Service), The Harvard Clinical and Translational Science Center (National Center for Advancing Translational Sciences, National Institutes of Health Award UL 1TR002541) and financial contributions from Harvard University and its affiliated academic healthcare centers. The content is solely the responsibility of the authors and does not necessarily represent the official views of Harvard Catalyst, Harvard University and its affiliated academic healthcare centers, or the National Institutes of Health.

Nonstandard Abbreviations and Acronyms:

C4KO	CITED4 Knockout
GO	Gene Ontology
GSEA	Gene Set Enrichment Analysis
KEGG	Kyoto Encyclopedia of Genes and Genomes
MEF	Mouse embryonic fibroblasts
miR/miRNA	Micro RNA
NRVF	Neonatal rat ventricular fibroblasts
NRVM	Neonatal rat ventricular myocytes
PE	Phenylephrine
siRNA	Small interfering RNA
TAC	Transverse aortic constriction

REFERENCES

1. Baggish AL. Mechanisms underlying the cardiac benefits of exercise: Still running in the dark. Trends in cardiovascular medicine. 2015;25:537–9. [PubMed: 25795335]
2. Guseh JS and Rosenzweig A. Size matters: Finding growth pathways that protect the heart. Cell research. 2017;27:1187–1188. [PubMed: 28925384]
3. Bostrom P, Mann N, Wu J, Quintero PA, Plovie ER, kova DP, Gupta RK, Xiao C, MacRae CA, Rosenzweig A and Spiegelman BM. C/EBPbeta Controls Exercise-Induced Cardiac Growth and Protects against Pathological Cardiac Remodeling. Cell. 2010;143:1072–1083 (*co-senior, co-corresponding, equal contributing authors). [PubMed: 21183071]
4. Yahata T, de Caestecker MP, Lechleider RJ, Andriole S, Roberts AB, Isselbacher KJ and Shioda T. The MSG1 non-DNA-binding transactivator binds to the p300/CBP coactivators, enhancing their functional link to the Smad transcription factors. The Journal of biological chemistry. 2000;275:8825–34. [PubMed: 10722728]
5. Shioda T, Lechleider RJ, Dunwoodie SL, Li H, Yahata T, de Caestecker MP, Fenner MH, Roberts AB and Isselbacher KJ. Transcriptional activating activity of Smad4: roles of SMAD hetero-oligomerization and enhancement by an associating transactivator. Proceedings of the National Academy of Sciences of the United States of America. 1998;95:9785–90. [PubMed: 9707553]
6. Ryall KA, Bezzerides VJ, Rosenzweig A and Saucerman JJ. Phenotypic screen quantifying differential regulation of cardiac myocyte hypertrophy identifies CITED4 regulation of myocyte elongation. Journal of molecular and cellular cardiology. 2014;72:74–84. [PubMed: 24613264]
7. Bezzerides VJ, Platt C, Lerchenmuller C, Paruchuri K, Oh NL, Xiao C, Cao Y, Mann N, Spiegelman BM and Rosenzweig A. CITED4 induces physiologic hypertrophy and promotes functional recovery after ischemic injury. JCI Insight. 2016;1.
8. Bostrom P, Mann N, Wu J, Quintero PA, Plovie ER, Panakova D, Gupta RK, Xiao C, MacRae CA, Rosenzweig A and Spiegelman BM. C/EBPbeta controls exercise-induced cardiac growth and protects against pathological cardiac remodeling. Cell. 2010;143:1072–83. [PubMed: 21183071]
9. Melman YF, Shah R, Danielson K, Xiao J, Simonson B, Barth A, Chakir K, Lewis GD, Lavender Z, Truong QA, Kleber A, Das R, Rosenzweig A, Wang Y, Kass D, Singh JP and Das S. Circulating MicroRNA-30d Is Associated With Response to Cardiac Resynchronization Therapy in Heart Failure and Regulates Cardiomyocyte Apoptosis: A Translational Pilot Study. Circulation. 2015;131:2202–2216. [PubMed: 25995320]
10. DeYoung MP, Horak P, Sofer A, Sgroi D and Ellisen LW. Hypoxia regulates TSC1/2-mTOR signaling and tumor suppression through REDD1-mediated 14–3-3 shuttling. Genes & development. 2008;22:239–51. [PubMed: 18198340]
11. Lin J, Handschin C and Spiegelman BM. Metabolic control through the PGC-1 family of transcription coactivators. Cell metabolism. 2005;1:361–70. [PubMed: 16054085]
12. Arany Z, Novikov M, Chin S, Ma Y, Rosenzweig A and Spiegelman BM. Transverse aortic constriction leads to accelerated heart failure in mice lacking PPAR-gamma coactivator 1alpha. Proceedings of the National Academy of Sciences of the United States of America. 2006;103:10086–91. [PubMed: 16775082]
13. Cunningham JT, Rodgers JT, Arlow DH, Vazquez F, Mootha VK and Puigserver P. mTOR controls mitochondrial oxidative function through a YY1-PGC-1alpha transcriptional complex. Nature. 2007;450:736–40. [PubMed: 18046414]
14. Xiao J, Gao R, Bei Y, Zhou Q, Zhou Y, Zhang H, Jin M, Wei S, Wang K, Xu X, Yao W, Xu D, Zhou F, Jiang J, Li X and Das S. Circulating miR-30d Predicts Survival in Patients with Acute Heart Failure. Cellular physiology and biochemistry : international journal of experimental cellular physiology, biochemistry, and pharmacology. 2017;41:865–874.
15. Duisters RF, Tijsen AJ, Schroen B, Leenders JJ, Lentink V, van der Made I, Herias V, van Leeuwen RE, Schellings MW, Barenbrug P, Maessen JG, Heymans S, Pinto YM and Creemers EE. miR-133 and miR-30 regulate connective tissue growth factor: implications for a role of microRNAs in myocardial matrix remodeling. Circulation research. 2009;104:170–8, 6p following 178. [PubMed: 19096030]

16. Fang L, Ellims AH, Moore XL, White DA, Taylor AJ, Chin-Dusting J and Dart AM. Circulating microRNAs as biomarkers for diffuse myocardial fibrosis in patients with hypertrophic cardiomyopathy. Journal of translational medicine. 2015;13:314. [PubMed: 26404540]
17. Mertins P, Udeshi ND, Clauser KR, Mani DR, Patel J, Ong SE, Jaffe JD and Carr SA. iTRAQ labeling is superior to mTRAQ for quantitative global proteomics and phosphoproteomics. Molecular & cellular proteomics : MCP. 2012;11:M111 014423.
18. GeneCards. https://www.genecards.org/cgi-bin/carddisp.pl?gene=MIR30D&keywords=mir30d accessed 01/02/2020.
19. Marsico A, Huska MR, Lasserre J, Hu H, Vucicevic D, Musahl A, Orom U and Vingron M. PROmiRNA: a new miRNA promoter recognition method uncovers the complex regulation of intronic miRNAs. Genome Biol. 2013;14:R84. [PubMed: 23958307]
20. Braganca J, Swingler T, Marques FI, Jones T, Eloranta JJ, Hurst HC, Shioda T and Bhattacharya S. Human CREB-binding protein/p300-interacting transactivator with ED-rich tail (CITED) 4, a new member of the CITED family, functions as a co-activator for transcription factor AP-2. The Journal of biological chemistry. 2002;277:8559–65. [PubMed: 11744733]
21. Hafner AV, Dai J, Gomes AP, Xiao C-Y, Palmeira CM, Rosenzweig A and Sinclair DA. Regulation of the mPTP by SIRT3-mediated deacetylation of CypD at lysine 166 suppresses age-related cardiac hypertrophy. Aging. 2010;2:1–10. [PubMed: 20228937]
22. Zhang D, Contu R, Latronico MV, Zhang J, Rizzi R, Catalucci D, Miyamoto S, Huang K, Ceci M, Gu Y, Dalton ND, Peterson KL, Guan KL, Brown JH, Chen J, Sonenberg N and Condorelli G. MTORC1 regulates cardiac function and myocyte survival through 4E-BP1 inhibition in mice. The Journal of clinical investigation. 2010;120:2805–16. [PubMed: 20644257]
23. Wencker D, Chandra M, Nguyen K, Miao W, Garantziotis S, Factor SM, Shirani J, Armstrong RC and Kitsis RN. A mechanistic role for cardiac myocyte apoptosis in heart failure. The Journal of clinical investigation. 2003;111:1497–504. [PubMed: 12750399]
24. Burke MA, Chang S, Wakimoto H, Gorham JM, Conner DA, Christodoulou DC, Parfenov MG, DePalma SR, Eminaga S, Konno T, Seidman JG and Seidman CE. Molecular profiling of dilated cardiomyopathy that progresses to heart failure. JCI insight. 2016;1.
25. Sciarretta S, Forte M, Frati G and Sadoshima J. New Insights Into the Role of mTOR Signaling in the Cardiovascular System. Circulation research. 2018;122:489–505. [PubMed: 29420210]
26. Simonson B, Subramanya V, Chan MC, Zhang A, Franchino H, Ottaviano F, Mishra MK, Knight AC, Hunt D, Ghiran I, Khurana TS, Kontaridis MI, Rosenzweig A and Das S. DDiT4L promotes autophagy and inhibits pathological cardiac hypertrophy in response to stress. Science signaling. 2017;10.
27. Martin ML and Blaxall BC. Cardiac intercellular communication: are myocytes and fibroblasts fair-weather friends? Journal of cardiovascular translational research. 2012;5:768–82. [PubMed: 23015462]
28. Chen S, Puthanveetil P, Feng B, Matkovich SJ, Dorn GW 2nd and Chakrabarti S. Cardiac miR-133a overexpression prevents early cardiac fibrosis in diabetes. Journal of cellular and molecular medicine. 2014;18:415–21. [PubMed: 24428157]
29. Matkovich SJ, Wang W, Tu Y, Eschenbacher WH, Dorn LE, Condorelli G, Diwan A, Nerbonne JM and Dorn GW 2nd. MicroRNA-133a protects against myocardial fibrosis and modulates electrical repolarization without affecting hypertrophy in pressure-overloaded adult hearts. Circulation research. 2010;106:166–75. [PubMed: 19893015]
30. Sassi Y, Avramopoulos P, Ramanujam D, Gruter L, Werfel S, Giosele S, Brunner AD, Esfandyari D, Papadopoulou AS, De Strooper B, Hubner N, Kumarswamy R, Thum T, Yin X, Mayr M, Laggerbauer B and Engelhardt S. Cardiac myocyte miR-29 promotes pathological remodeling of the heart by activating Wnt signaling. Nature communications. 2017;8:1614.
31. van Rooij E, Sutherland LB, Thatcher JE, DiMaio JM, Naseem RH, Marshall WS, Hill JA and Olson EN. Dysregulation of microRNAs after myocardial infarction reveals a role of miR-29 in cardiac fibrosis. Proceedings of the National Academy of Sciences of the United States of America. 2008;105:13027–32. [PubMed: 18723672]
32. Cavarretta E and Condorelli G. miR-21 and cardiac fibrosis: another brick in the wall? European heart journal. 2015;36:2139–41. [PubMed: 25975660]

33. Thum T, Gross C, Fiedler J, Fischer T, Kissler S, Bussen M, Galuppo P, Just S, Rottbauer W, Frantz S, Castoldi M, Soutschek J, Koteliansky V, Rosenwald A, Basson MA, Licht JD, Pena JT, Rouhanifard SH, Muckenthaler MU, Tuschl T, Martin GR, Bauersachs J and Engelhardt S. MicroRNA-21 contributes to myocardial disease by stimulating MAP kinase signalling in fibroblasts. Nature. 2008;456:980–4. [PubMed: 19043405]
34. Deng S, Zhao Q, Zhen L, Zhang C, Liu C, Wang G, Zhang L, Bao L, Lu Y, Meng L, Lu J, Yu P, Lin X, Zhang Y, Chen YH, Fan H, Cho WC, Liu Z and Yu Z. Neonatal Heart-Enriched miR-708 Promotes Proliferation and Stress Resistance of Cardiomyocytes in Rodents. Theranostics. 2017;7:1953–1965. [PubMed: 28638481]
35. Pan Z, Sun X, Shan H, Wang N, Wang J, Ren J, Feng S, Xie L, Lu C, Yuan Y, Zhang Y, Wang Y, Lu Y and Yang B. MicroRNA-101 inhibited postinfarct cardiac fibrosis and improved left ventricular compliance via the FBJ osteosarcoma oncogene/transforming growth factor-beta1 pathway. Circulation. 2012;126:840–50. [PubMed: 22811578]
36. Bayindir-Buchhalter I, Wolff G, Lerch S, Sijmonsma T, Schuster M, Gronych J, Billeter AT, Babaei R, Krunic D, Ketscher L, Spielmann N, Hrabe de Angelis M, Ruas JL, Muller-Stich BP, Heikenwalder M, Lichter P, Herzig S and Vegiopoulos A. Cited4 is a sex-biased mediator of the antidiabetic glitazone response in adipocyte progenitors. EMBO molecular medicine. 2018.
37. Abel ED, Kaulbach HC, Tian R, Hopkins JC, Duffy J, Doetschman T, Minnemann T, Boers ME, Hadro E, Oberste-Berghaus C, Quist W, Lowell BB, Ingwall JS and Kahn BB. Cardiac hypertrophy with preserved contractile function after selective deletion of GLUT4 from the heart. The Journal of clinical investigation. 1999;104:1703–14. [PubMed: 10606624]
38. Fliegner D, Schubert C, Penkalla A, Witt H, Kararigas G, Dworatzek E, Staub E, Martus P, Ruiz Noppinger P, Kintscher U, Gustafsson JA and Regitz-Zagrosek V. Female sex and estrogen receptor-beta attenuate cardiac remodeling and apoptosis in pressure overload. American journal of physiology Regulatory, integrative and comparative physiology. 2010;298:R1597–606.
39. Taniike M, Yamaguchi O, Tsujimoto I, Hikoso S, Takeda T, Nakai A, Omiya S, Mizote I, Nakano Y, Higuchi Y, Matsumura Y, Nishida K, Ichijo H, Hori M and Otsu K. Apoptosis signal-regulating kinase 1/p38 signaling pathway negatively regulates physiological hypertrophy. Circulation. 2008;117:545–52. [PubMed: 18195174]
40. Collins KA, Korcarz CE, Shroff SG, Bednarz JE, Fentzke RC, Lin H, Leiden JM and Lang RM. Accuracy of echocardiographic estimates of left ventricular mass in mice. American journal of physiology Heart and circulatory physiology. 2001;280:H1954–62. [PubMed: 11299194]
41. Vernochet C, Damilano F, Mourier A, Bezy O, Mori MA, Smyth G, Rosenzweig A, Larsson NG and Kahn CR. Adipose tissue mitochondrial dysfunction triggers a lipodystrophic syndrome with insulin resistance, hepatosteatosis, and cardiovascular complications. FASEB journal : official publication of the Federation of American Societies for Experimental Biology. 2014;28:4408–19. [PubMed: 25005176]
42. Graham EL, Balla C, Franchino H, Melman Y, del Monte F and Das S. Isolation, culture, and functional characterization of adult mouse cardiomyoctyes. Journal of visualized experiments : JoVE. 2013:e50289. [PubMed: 24084584]
43. Liu X, Xiao J, Zhu H, Wei X, Platt C, Damilano F, Xiao C, Bezzerides V, Bostrom P, Che L, Zhang C, Spiegelman BM and Rosenzweig A. miR-222 is necessary for exercise-induced cardiac growth and protects against pathological cardiac remodeling. Cell metabolism. 2015;21:584–95. [PubMed: 25863248]
44. Irizarry RA, Bolstad BM, Collin F, Cope LM, Hobbs B and Speed TP. Summaries of affymetrix GeneChip probe level data. Nucleic Acids Res. 2003;31.
45. Bolstad BM, Irizarry RA, Astrand M and Speed TP. A comparison of normalization methods for high density oligonucleotide array data based on variance and bias. Bioinformatics. 2003;19:185–193. [PubMed: 12538238]
46. Irizarry RA, Hobbs B, Collin F, Beazer-Barclay YD, Antonellis KJ, Scherf U and Speed TP. Exploration, normalization, and summaries of high density oligonucleotide array probe level data. Biostatistics. 2003;4:249–264. [PubMed: 12925520]
47. Carvalho BS and Irizarry RA. A framework for oligonucleotide microarray preprocessing. Bioinformatics. 2010;26:2363–2367. [PubMed: 20688976]

48. Ritchie ME, Phipson B, Wu D, Hu YF, Law CW, Shi W and Smyth GK. limma powers differential expression analyses for RNA-sequencing and microarray studies. Nucleic Acids Res. 2015;43.
49. Mootha VK, Lindgren CM, Eriksson KF, Subramanian A, Sihag S, Lehar J, Puigserver P, Carlsson E, Ridderstrale M, Laurila E, Houstis N, Daly MJ, Patterson N, Mesirov JP, Golub TR, Tamayo P, Spiegelman B, Lander ES, Hirschhorn JN, Altshuler D and Groop LC. PGC-1 alpha-responsive genes involved in oxidative phosphorylation are coordinately downregulated in human diabetes. Nat Genet. 2003;34:267–273. [PubMed: 12808457]
50. Subramanian A, Tamayo P, Mootha VK, Mukherjee S, Ebert BL, Gillette MA, Paulovich A, Pomeroy SL, Golub TR, Lander ES and Mesirov JP. Gene set enrichment analysis: A knowledge-based approach for interpreting genome-wide expression profiles. Proceedings of the National Academy of Sciences of the United States of America. 2005;102:15545–15550. [PubMed: 16199517]
51. Danielson KM, Shah R, Yeri A, Liu X, Camacho Garcia F, Silverman M, Tanriverdi K, Das A, Xiao C, Jerosch-Herold M, Heydari B, Abbasi S, Van Keuren-Jensen K, Freedman JE, Wang YE, Rosenzweig A, Kwong RY and Das S. Plasma Circulating Extracellular RNAs in Left Ventricular Remodeling Post-Myocardial Infarction. EBioMedicine. 2018;32:172–181. [PubMed: 29779700]
52. Martin M Cutadapt removes adapter sequences from high-throughput sequencing reads. EMBnetjournal (Internet). 2011;2011;17:10.
53. Langmead B, Trapnell C, Pop M and Salzberg SL. Ultrafast and memory-efficient alignment of short DNA sequences to the human genome. Genome Biol. 2009;10.
54. Dobin A, Davis CA, Schlesinger F, Drenkow J, Zaleski C, Jha S, Batut P, Chaisson M and Gingeras TR. STAR: ultrafast universal RNA-seq aligner. Bioinformatics. 2013;29:15–21. [PubMed: 23104886]
55. Kozomara A and Griffiths-Jones S. miRBase: annotating high confidence microRNAs using deep sequencing data. Nucleic Acids Res. 2014;42:D68–D73. [PubMed: 24275495]
56. Chan PP and Lowe TM. GtRNAdb: a database of transfer RNA genes detected in genomic sequence. Nucleic Acids Res. 2009;37:D93–D97. [PubMed: 18984615]
57. Zhang P, Si XH, Skogerbo G, Wang JJ, Cui DY, Li YX, Sun XB, Liu L, Sun BF, Chen RS, He SM and Huang DW. piRBase: a web resource assisting piRNA functional study. Database-Oxford. 2014.
58. Love MI, Huber W and Anders S. Moderated estimation of fold change and dispersion for RNA-seq data with DESeq2. Genome Biol. 2014;15.
59. Yeri A, Courtright A, Danielson K, Hutchins E, Alsop E, Carlson E, Hsieh M, Ziegler O, Das A, Shah RV, Rozowsky J, Das S and Van Keuren-Jensen K. Evaluation of commercially available small RNASeq library preparation kits using low input RNA. BMC genomics. 2018;19:331. [PubMed: 29728066]
60. Robinson JT, Thorvaldsdottir H, Winckler W, Guttman M, Lander ES, Getz G and Mesirov JP. Integrative genomics viewer. Nat Biotechnol. 2011;29:24–6. [PubMed: 21221095]
61. Patro R, Duggal G, Love MI, Irizarry RA and Kingsford C. Salmon provides fast and bias-aware quantification of transcript expression. Nature methods. 2017;14:417–419. [PubMed: 28263959]
62. Patten RDfA. Subcellular Fractionation Protocol. 2020.
63. Ikeda Y, Shirakabe A, Maejima Y, Zhai P, Sciarretta S, Toli J, Nomura M, Mihara K, Egashira K, Ohishi M, Abdellatif M and Sadoshima J. Endogenous Drp1 mediates mitochondrial autophagy and protects the heart against energy stress. Circulation research. 2015;116:264–78. [PubMed: 25332205]
64. Spurr AR. A low-viscosity epoxy resin embedding medium for electron microscopy. Journal of ultrastructure research. 1969;26:31–43. [PubMed: 4887011]
65. Venable JH and Coggeshall R. A Simplified Lead Citrate Stain for Use in Electron Microscopy. The Journal of cell biology. 1965;25:407–8. [PubMed: 14287192]

NOVELTY AND SIGNIFICANCE

What Is Known?

- Exercise promotes cardiovascular health and mitigates established disease.
- Regular exercise leads to physiological cardiac growth, while diseases like hypertension and aortic stenosis, for example, lead to pathological growth.
- CITED4 is part of a gene program induced by exercise and is sufficient to cause physiological cardiac growth, mimicking the exercise response of the heart, and can mitigate adverse cardiac remodeling after ischemic injury.

What New Information Does This Article Contribute?

- CITED4 is upregulated in both physiological and pathological cardiac growth and is necessary to prevent adverse remodeling in both settings.
- Cardiomyocyte CITED4 knockout (C4KO) leads to rapid heart failure characterized by ventricular dilation, apoptosis, autophagy, and cardiac fibrosis in a murine model of pathological cardiac growth.
- CITED4 protects against pathological cardiac remodeling by regulating mTOR (mammalian target of rapamycin) activity and a network of miRNAs mediating cardiomyocyte to fibroblast crosstalk

Although the beneficial preventive and therapeutic effects of exercise are well established, the underlying molecular mechanisms are not well understood. Cardiac CITED4 was previously shown to be induced by exercise and sufficient to cause physiological hypertrophy and mitigate adverse remodeling after ischemic injury. However, the role of endogenous CITED4 in response to physiological or pathological stress was unknown. We investigated the role of CITED4 using a cardiomyocyte-specific knockout model. We found that CITED4 increased not only in response to exercise but also in response to pathological stress, making it a notable exception to the general rule that the pathways involved in physiological and pathological growth of the heart are largely distinct. While cardiac morphology and function were normal at baseline in young adult C4KO mice, they manifested a maladaptive response to exercise. After pressure overload, C4KO mice showed impaired cardiac hypertrophy, decreased activation of mTOR and mitochondrial signaling, increased autophagy, apoptosis, and fibrosis. CITED4 regulates a network of pro-fibrotic miRNAs, and one of these, miR30d, appeared to mediate cardiomyocyte-fibroblast cross talk dependent on CITED4. These data demonstrate that CITED4 is upregulated in both pathological and physiological remodeling and in both settings protects against maladaptive remodeling.

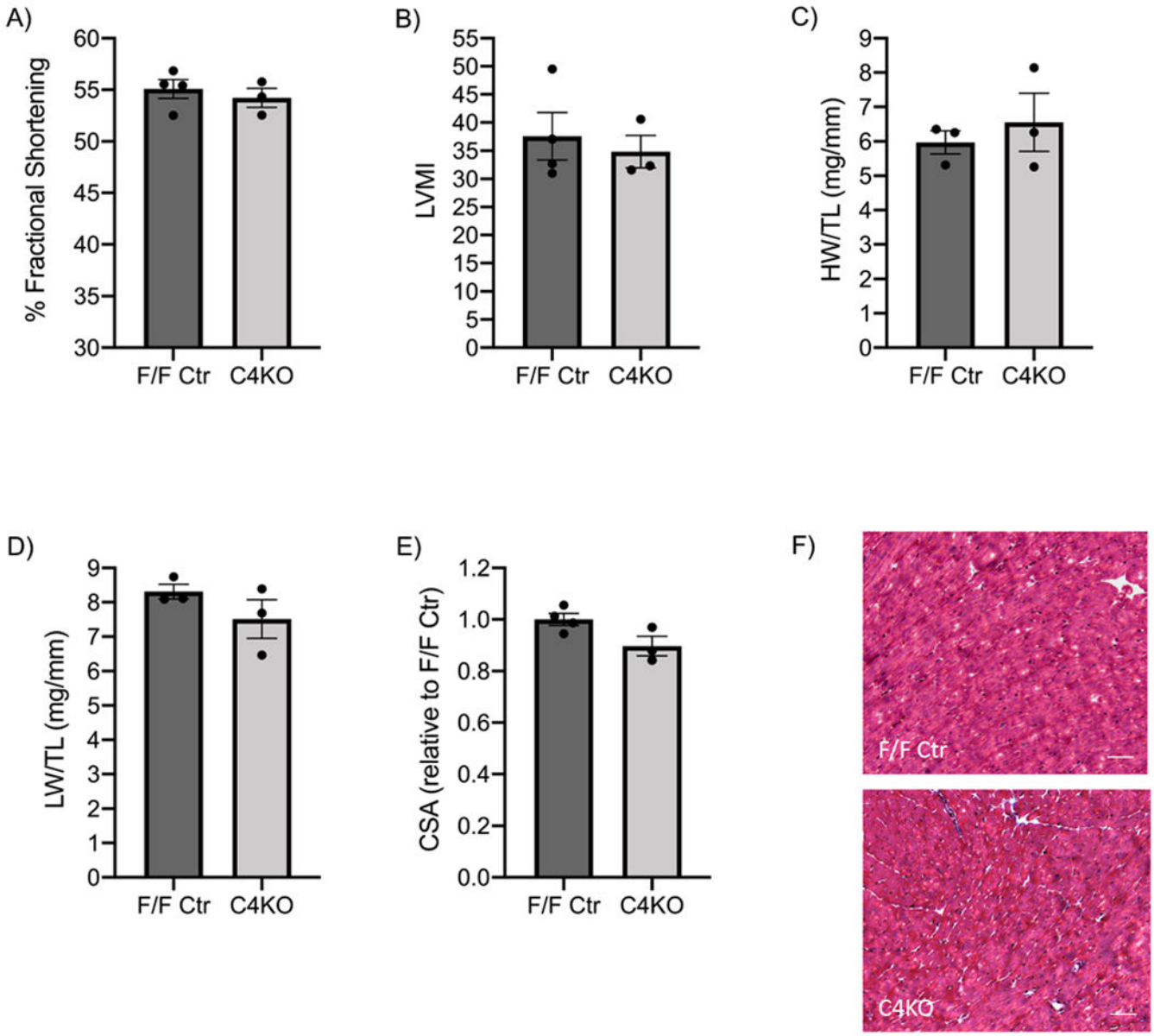

Figure 1: Cardiomyocyte specific CITED4 knockout does not affect baseline cardiac mass or function in young adult mice.

A, Baseline Fractional Shortening (%FS) in C4KO compared to F/F Ctr mice in 8-12 week old mice (n=4 F/F Ctr, 3 C4KO, p=0.54). **B**, Left ventricular mass index (LVMI) for C4KO and control animals (n=4 F/F Ctr, 3 C4KO, p=0.64). **C**, Heart weight to tibia length ratios (HW/TL) in C4KO and F/F Ctr animals (n= 3 mice per group, p=0.56). **D**, Lung weight to tibia length ratios (LW/TL) in C4KO and F/F Ctr animals (n=3 mice per group), p=0.25). **E**, Cross sectional area (CSA) of C4KO relative to F/F Ctr cardiomyocytes at baseline (n=4 F/F Ctr, 3 C4KO, p=0.057). **F**, Micrographs of cardiac sections stained with Masson Trichrome Staining used to measure cross sectional area in E, scale bar = 75μm, images were chosen to represent average of both groups. For all graphs significance was determined by Student's t-test, *p<0.05.

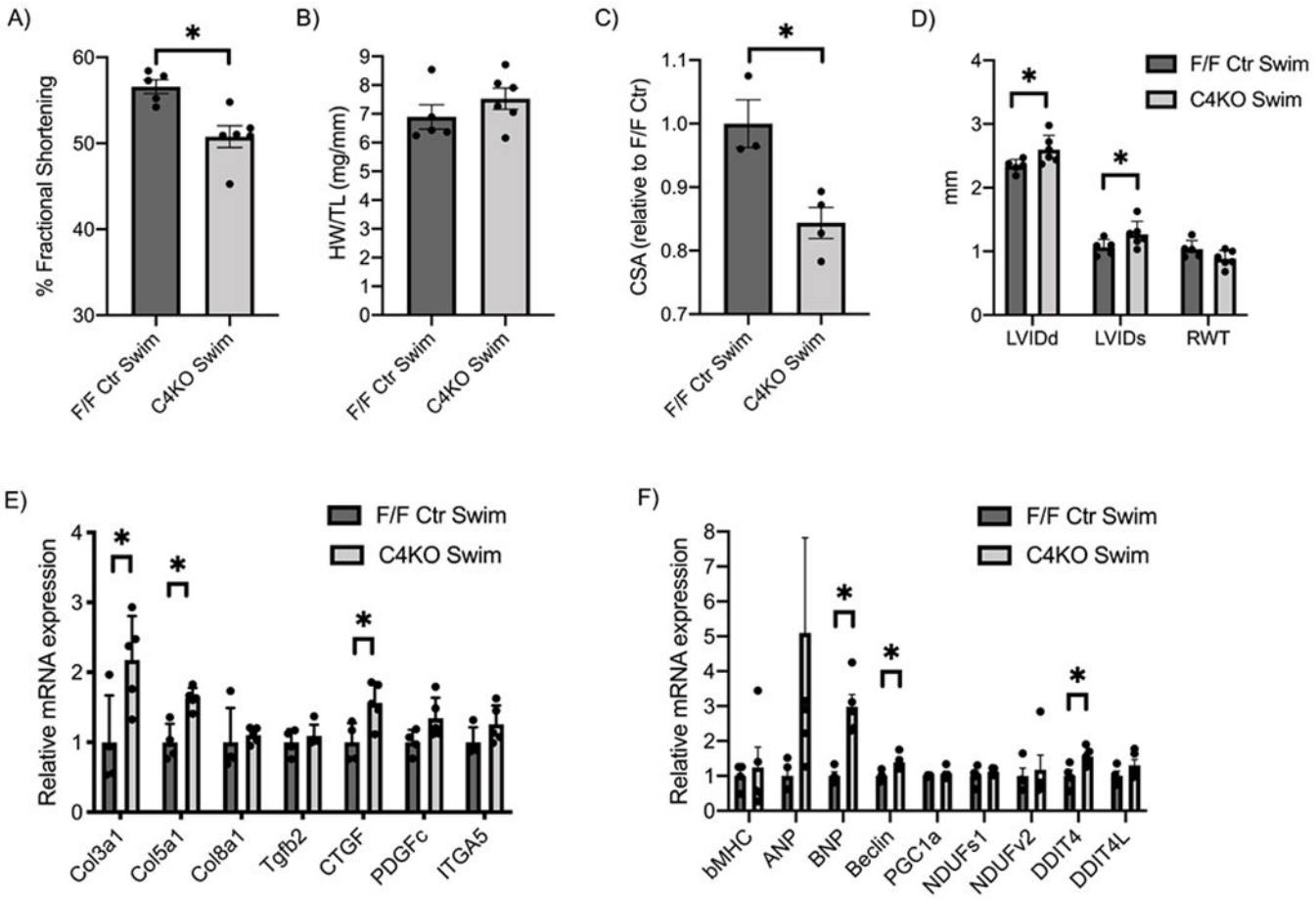

Figure 2: Cardiomyocyte specific deletion of CITED4 causes maladaptive remodeling and a functional deficit in response to endurance exercise.

A, Fractional Shortening (%FS) in C4KO compared to F/F Ctr mice after swimming exercise (n=5 F/F Ctr, 6 C4KO, p=0.005). **B**, Heart weight to tibia length ratios (HW/TL) in C4KO and F/F Ctr animals (n=5 F/F Ctr, 6 C4KO, p=0.29) after swimming exercise. **C,** Cross sectional area (CSA) of C4KO relative to F/F Ctr cardiomyocytes at baseline (n=3 F/F Ctr, 4 C4KO, p=0.015). **D**, Left ventricular internal dimension in end-diastole (LVIDd, p=0.043) and end-systole (LVIDs, p=0.049) as well as relative wall thickness (RWT, p=0.097) assessed by echocardiography in C4KO and control animals after swimming exercise (n=5 F/F Ctr, 6 C4KO). **E**, qPCR analysis of fibrosis-related genes in C4KO relative to F/F Ctr hearts after swimming exercise (Col3a1 p<0.001, Col5a1 p=0.008, CTGF p=0.017. **F**, qPCR analysis related to physiological and pathological remodeling (bMHC, ANP, BNP p=0.002), autophagy (Beclin1 p=0.023) and mitochondrial pathways (PGC1a, NDUFs1, NDUFv2) and mTOR regulators (DDIT4 p=0.027, DDIT4L) in C4KO relative to F/F Ctr hearts after swimming exercise (n=4 F/F Ctr, 5 C4KO). For all graphs significance was determined by Student's t-test, *p<0.05.

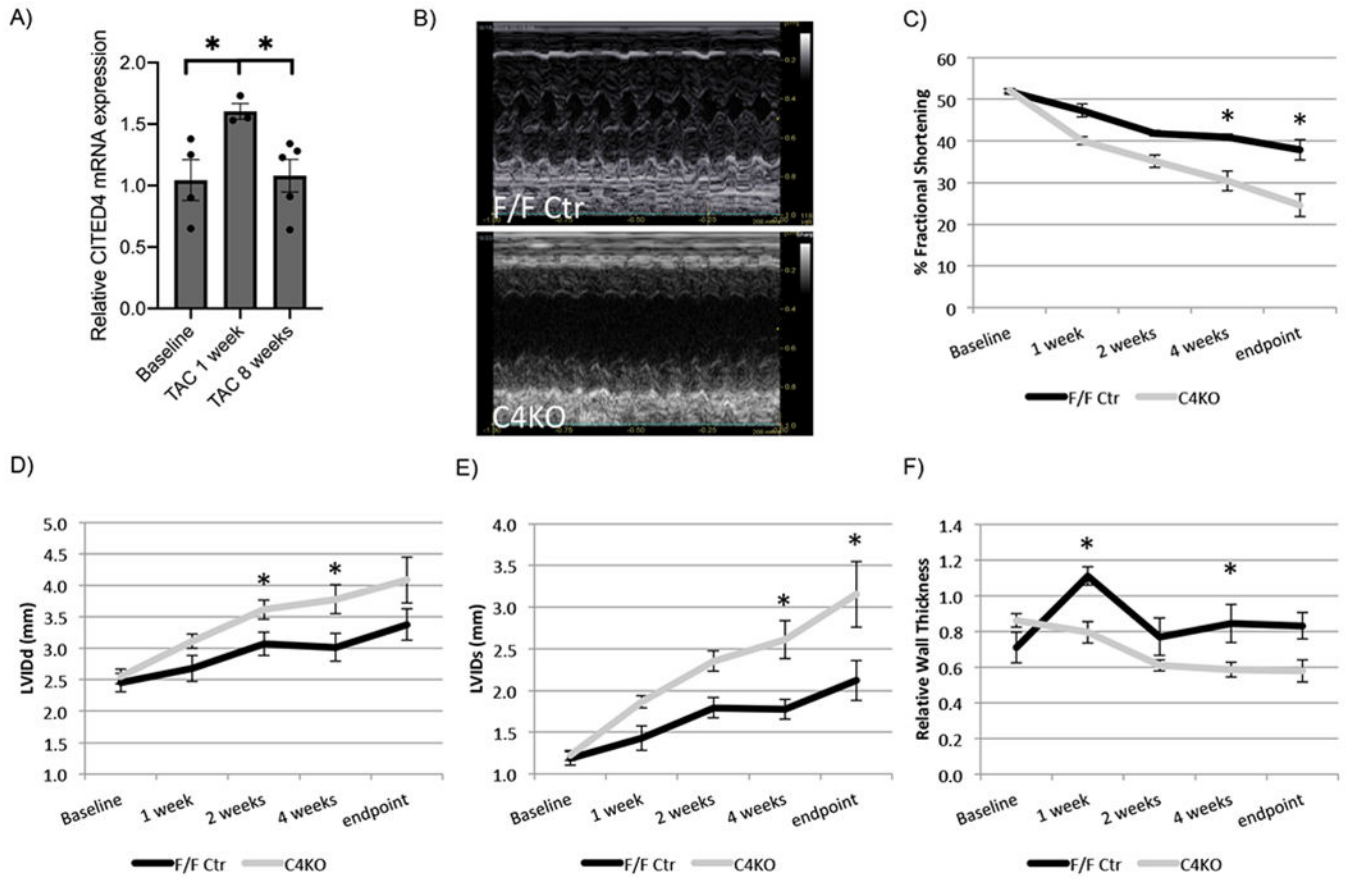

Figure 3: Cardiomyocyte specific CITED4 knockout mice develop accelerated heart failure after transverse aortic constriction (TAC).

A, qPCR analysis of CITED4 mRNA in hearts of control mice at 1 week (n=3) and 8 weeks (n=5) after TAC and at baseline (n=4) (p<0.035 baseline vs. 1 week, p<0.028 1 week vs. 8 weeks, p=0.874 baseline vs. 8 weeks, one-way ANOVA with Sidak's multiple comparisons test). **B,** Echocardiographic images from F/F Ctr and C4KO 8 weeks after TAC, images were chosen to represent average of both groups. **C**, Assessment of ventricular function by echocardiography in C4KO compared to F/F Ctr mice at indicated time points before and after TAC surgery (n=6 F/F Ctr, 6 C4KO, p=.999, 0.050, 0.064, 0.002, <0.001, respectively). **D**, Left ventricular dimensions in end-diastole (LVIDd, p=0.999, 0.245, 0.009, 0.025, 0.282, respectively) and **E**, end-systole (LVIDs) at indicated time points before and after TAC surgery (n=6 F/F Ctr, 6 C4KO, p=0.999, 0.426, 0.076, 0.017, <0.0001, respectively). **F**, Relative wall thickness assessed by echocardiography in C4KO and control animals at indicated time points before and after TAC surgery (n=6 F/F Ctr, 6 C4KO, p=0.998, 0.026, 0.391, 0.049, <0.607, respectively). For all graphs in C-F significance was determined by repeated-measures two-way ANOVA and Sidak's multiple comparisons test, *p<0.05.

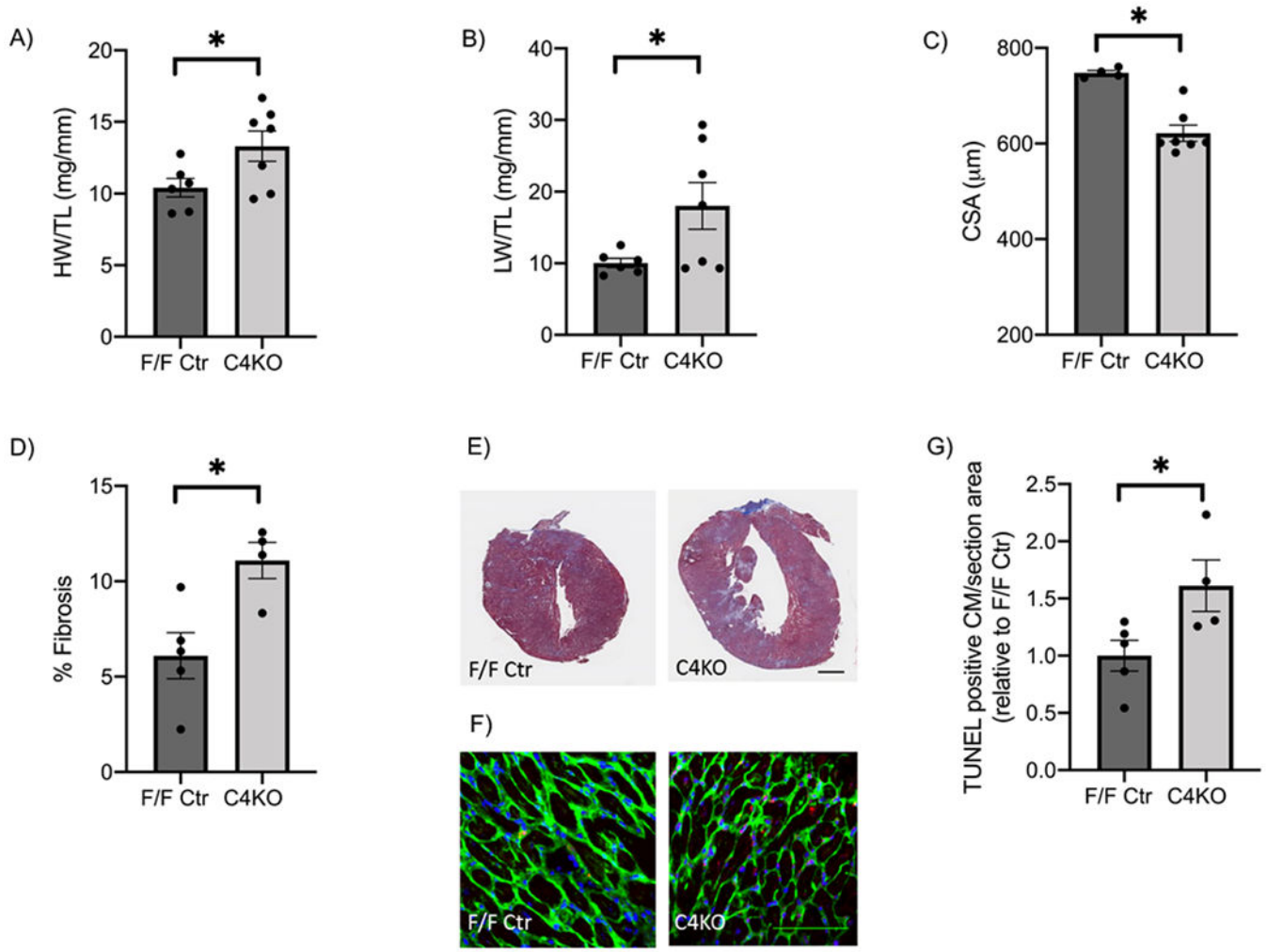

Figure 4: Cardiomyocyte specific CITED4 knockout mice develop ventricular dilation and maladaptive remodeling in response to pressure overload.

A, Heart weight to tibia length ratios (HW/TL) in C4KO and F/F Ctr animals at endpoint after TAC surgery (n=6 F/F Ctr, 7 C4KO, p=0.046). **B**, Lung weight to tibia length ratios (LW/TL) in C4KO and F/F Ctr animals at endpoint after TAC surgery (n=6 F/F Ctr, 7 C4KO, p=0.049). **C**, Cross sectional area measurement from C4KO compared to F/F Ctr hearts at endpoint after TAC surgery (n=4 F/F Ctr, 7 C4KO, >200 cells per section, p<0.001). **D**, Quantification of fibrosis measured as percentage of total myocardial area in C4KO compared to F/F Ctr hearts at the endpoint after TAC surgery (n=5 F/F Ctr, 4 C4KO, p=0.017). **E**, Micrographs of cardiac sections stained with Masson Trichrome Staining to label fibrotic tissue one week after TAC surgery, scale bar = 1mm, images were chosen to represent differences of fibrosis pattern in both groups. **F**, Images of TUNEL staining in C4KO compared to F/F Ctr hearts one week after TAC surgery. Sections were stained with Wheat Germ Agglutinin (WGA) to mark cellular membranes (green), TUNEL (red), and DAPI (blue), scale bar=100µm, images were chosen to represent TUNEL positive areas in both groups. **G**, Quantification of TUNEL-positive cardiomyocytes in C4KO relative to F/F

Ctr hearts one week after TAC surgery (n=5 F/F Ctr, 4 C4KO, p=0.044). For all graphs significance was determined by Student's t-test, *p<0.05 unless indicated otherwise.

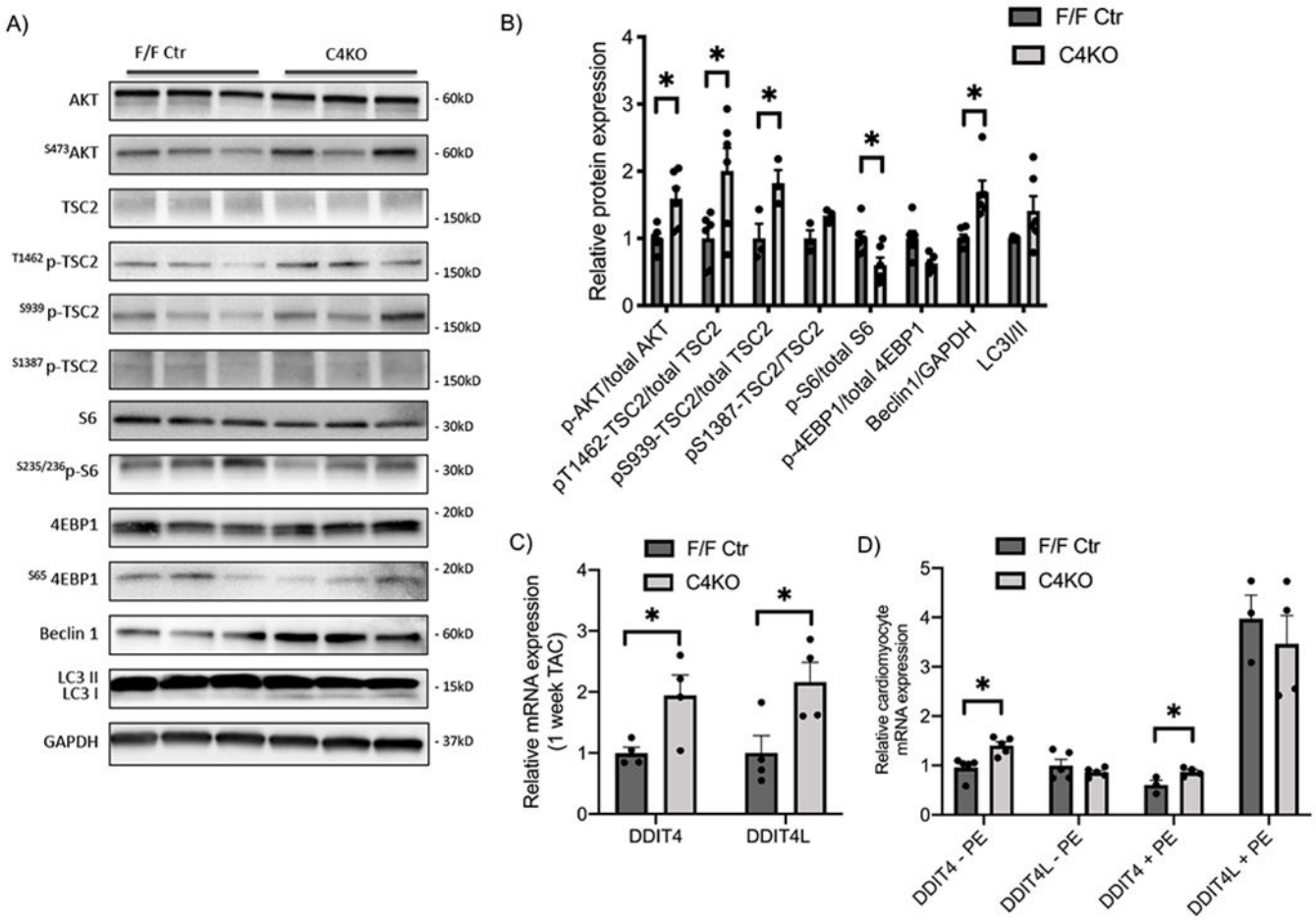

Figure 5: mTOR signaling is impaired in C4KO hearts after pressure overload.

A, Western Blot of protein isolated from heart lysates one week after TAC surgery comparing AKT, TSC2, S6- and 4EBP-protein-phosphorylation and Beclin1 and LC3 protein expression in C4KO hearts with F/F Ctr hearts. GAPDH served as protein loading control. **B**, Quantification of AKT (p=0.008), T1462-TSC2 (p=0.024), S939-TSC2 (p=0.047), S1387-TSC2 (p=0.063), pS6 (p=0.026) and p4EBP (p=0.012) protein-phosphorylation and Beclin1 (p=0.003) and LC3 A/B (p=0.087) protein expression in C4KO hearts relative to F/F Ctr hearts one week after TAC (n=6 F/F Ctr, 6 C4KO, *p<0.05, Student's t-test). **C**, qPCR analysis of mTORC1 inhibitors REDD1 (DDIT4) and REDD2 (DDIT4L) in C4KO relative to F/F Ctr hearts one week after TAC surgery (n=4/group, *p=0.032 and 0.023, respectively, Student's t-test). **D**, qPCR analysis of REDD1 (DDIT4) and REDD2 (DDIT4L) mRNA expression in isolated ventricular myocytes from F/F Ctr and C4KO hearts at baseline (n=5/group, p=0.029 REDD1 and 0.799 for REDD2) and after Phenylephrine (PE) stimulation (n=4 F/F Ctr, 3 C4KO, *p=0.002 for REDD1 −PE, 0.035 +PE, ns for REDD2, *p<0.05 one-way ANOVA and Sidak's post test).

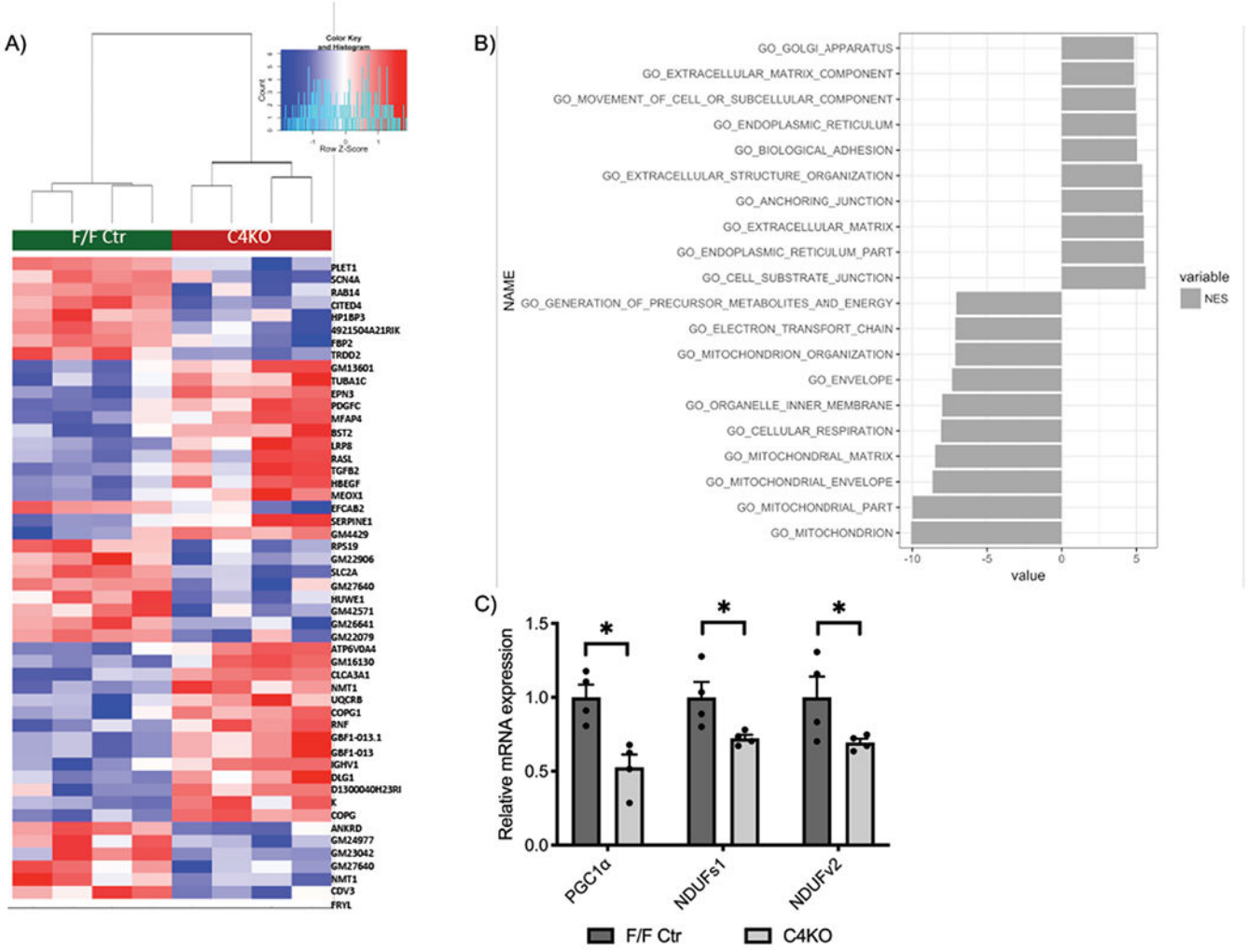

Figure 6: Gene expression array reveals impaired mitochondrial pathways in C4KO hearts after pressure overload.

A, Heatmap depicts differentially expressed mRNA (applying the combined criteria of p≤0.005 and fold change ≥1.5) in C4KO and F/F Ctr heart samples (n=4/group) one week after TAC surgery. The dendrogram was constructed using the Manhattan-Ward clustering algorithm. **B**, Bar-plot of the top 10 most significantly enriched pathways, Gene Set Enrichment Analysis (GSEA) using Gene Ontology database. Bars depict the normalized enrichment score of pathway up- or downregulation in C4KO hearts relative to F/F Ctr hearts one week after TAC surgery (n=4/group). **C**, qPCR for validation of reduced PGC1α, NDUFs1, and NDUFv2 mRNA expression (n=4 F/F Ctr, 4 C4KO, p=0.001, 0.039, 0.024, respectively), Student's t-test, *p<0.05.

A)

miRNA	logFC
mmu-miR-495-5p	0.72458308967318
mmu-miR-708-5p	-0.67993718354358
mmu-miR-21a-3p	0.647158502384336
mmu-miR-543-3p	0.541482347398593
mmu-miR-30a-5p	-0.50235526268483
mmu-miR-700-3p	-0.618012425679382
mmu-miR-3154	0.521906221545675
mmu-miR-133a-3p	-0.406139903085544
mmu-miR-223-5p	0.50880470104762
mmu-miR-133b-3p	-0.465640163003332
mmu-miR-378a-5p	-0.501901259644146
mmu-miR-29c-5p	-0.333822656569614
mmu-miR-30e-5p	-0.490102439946416
mmu-miR-101a-5p	-0.525808052450932
mmu-miR-376b-5p	0.405604542832002
mmu-miR-30d-5p	-0.432821384512756
mmu-miR-431-5p	0.477803750134881
mmu-miR-1247-3p	0.555758419869098
mmu-miR-376c-3p	0.501393177162485
mmu-miR-181c-3p	-0.383189832131867
mmu-miR-708-3p	-0.557683146052032
mmu-miR-29c-3p	-0.446887776179245
mmu-miR-299a-3p	0.478019092139192
mmu-miR-30c-1-3p	-0.42033335122237
mmu-miR-137-3p	0.548284705258878
mmu-miR-136-3p	0.398104796115735
mmu-miR-378a-3p	-0.439401529698833
mmu-miR-212-3p	-0.2992924977813
mmu-miR-154-3p	0.486050979409388
mmu-miR-434-3p	0.4518043343694
mmu-miR-134-5p	0.444863938925111
mmu-miR-410-3p	0.481448438189094

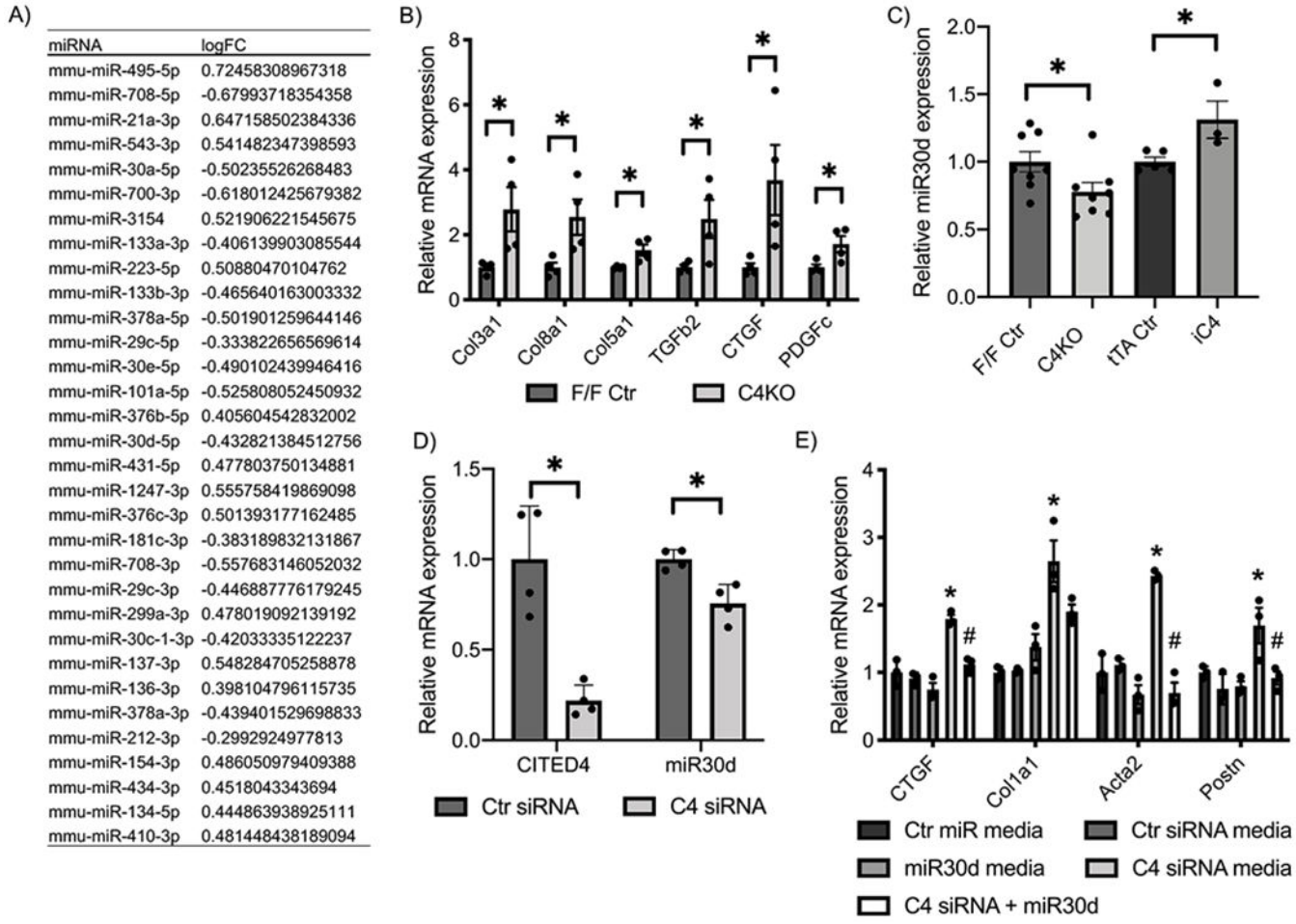

Figure 7: Fibrosis-related pathways are dysregulated in C4KO hearts after pressure overload.

A, Differentially expressed, fibrosis-related (annotated and/or published) miRNAs in C4KO compared to F/F Ctr hearts one week after TAC surgery assessed by miRNASeq profiling (n= 5/group). **B**, qPCR validation of fibrosis-related genes (mRNA) inversely regulated by differentially expressed miRNAs (A) in C4KO relative to F/F Ctr hearts after TAC surgery (n=4/group, p=0.041, 0.033, 0.021, 0.045, 0.048, 0.036, respectively, *p<0.05, Student's t-test). **C**, qPCR validation of miR-30d expression in C4KO relative to F/F Ctr hearts one week after TAC surgery (n=8/group, p=0.045) and in hearts from inducible CITED4 mice relative to tTA Ctr hearts (n=4/group, p=0.029), *p<0.05, Student's t-test. **D**, Neonatal rat ventricular myocytes (NRVM) were treated with negative control (Ctr) and CITED4 (C4) siRNA. C4 siRNA treatment lead to a reproducible decrease in CITED4 mRNA expression (p=0.002) and caused a decrease in miR30d expression (p=0.006) (n=4 individual experiments, *p<0.05, Student's t-test). **E**, CTGF (*p<0.001, $^{\#}p$<0.001, Ctr miR vs. C4 siRNA p=0.002), Col1a1 (*p<0.001, Ctr miR vs. C4 siRNA p<0.001, p=0.039 Ctr miR vs. C4+miR30d, miR30d vs. C4 siRNA p=0.037), Acta2 (*p<0.001, $^{\#}p$<0.001, miR30d vs. C4 siRNA p<0.001) and Postn (*p=0.010, $^{\#}p$=0.033, miR30d vs. C4 siRNA p=0.014) mRNA expression evaluated in mouse embryonic fibroblasts (MEF) that were either treated with conditioned media from Ctr siRNA, Ctr miRNA mimic or C4 siRNA, miR30d mimic, or C4

siRNA in addition to miR30d mimic NRVMs (n=3 individual experiments, *p<0.05 vs. Ctr siRNA and Ctr miR, $^{\#}p$<0.05 vs. C4 siRNA, one-way ANOVA and Sidak's post test).

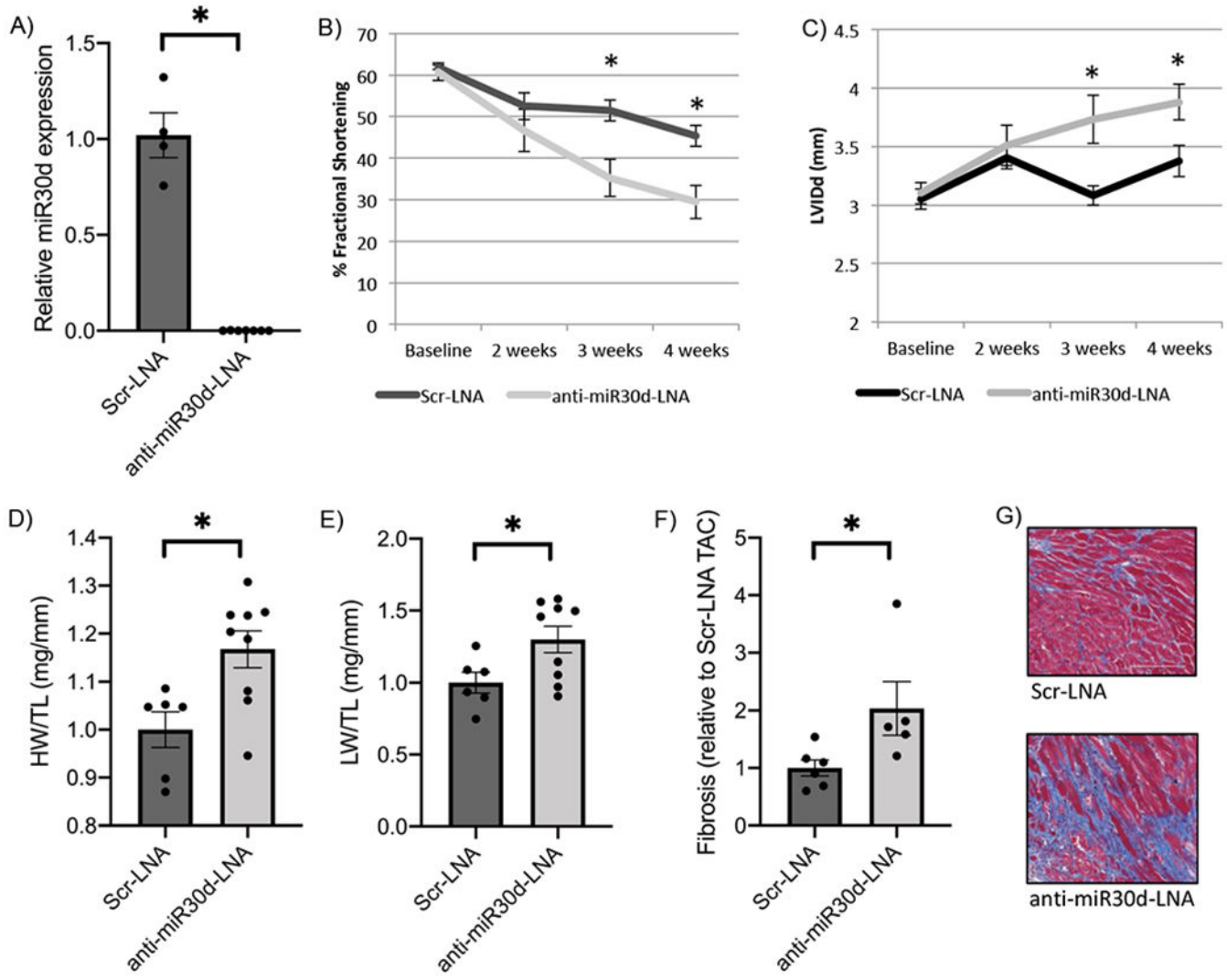

Figure 8: LNA mediated miR30d depletion leads to rapid cardiac failure and fibrosis in response to pressure overload.

A, Confirmation of successful locked nucleic acid (LNA) mediated miR30d depletion, relative miR30d expression in heart lysates from LNA-anti-miR30d and scramble (Scr) control LNA treated mice (n=4 Scr-LNA, 7 LNA-anti-miR30d, Student's t-test, $p<0.001$, $*p<0.05$). **B**, Assessment of ventricular function by echocardiography in LNA-anti-miR30d compared to Scr-LNA treated mice at indicated time points before and after TAC surgery (n=6 Scr-LNA, 6 LNA-anti-miR30d, $p=0.999$, 0.999, 0.035, 0.033, respectively, repeated-measures two-way ANOVA with Sidak's post test for multiple comparisons, $*p<0.05$). **C**, Left ventricular dimensions in end-diastole (LVIDd) at indicated time points before and after TAC surgery (n=6 Scr-LNA, 6 LNA-anti-miR30d, $p=0.999$, 0.922, 0.037, 0.034, respectively, repeated-measures two-way ANOVA with Sidak's post test for multiple comparisons, $*p<0.05$). **D**, Heart weight to tibia length ratios (HW/TL) in LNA-anti-miR30d and Scr-LNA treated animals 4 weeks after TAC surgery (n=6 Scr-LNA, 9 LNA-anti-miR30d, Student's t-test, $p=0.010$, $*p<0.05$). **E**, Lung weight to tibia length ratios (LW/TL) in LNA-anti-miR30d and Scr-LNA treated animals 4 weeks after TAC surgery (n=6 Scr-

LNA, 9 LNA-anti-miR30d, Student's t-test, p=0.036, *p<0.05). **F**, Quantification of fibrosis measured as percentage of total myocardial area in LNA-anti-miR30d compared to Scr-LNA treated hearts 4 weeks after TAC surgery (n=6 Scr-LNA, 5 LNA-anti-miR30d, Student's t-test, p=0.047, *p<0.05) **G**, Micrographs of cardiac sections stained with Masson Trichrome Staining to label fibrotic tissue 4 weeks after TAC surgery, scale bar=100μm, images were chosen to represent differences of fibrosis pattern in both groups.